

We are committed to providing [accessible customer service](#).

If you need accessible formats or communications supports, please [contact us](#).

Nous tenons à améliorer [l'accessibilité des services à la clientèle](#).

Si vous avez besoin de formats accessibles ou d'aide à la communication, veuillez [nous contacter](#).

VTEM™ plus



TECHNICAL REPORT ON A HELICOPTER-BORNE VERSATILE TIME DOMAIN ELECTROMAGNETIC (VTEM™ plus) AND HORIZONTAL MAGNETIC GRADIOMETER GEOPHYSICAL SURVEY

AUTHORS:

Nick Venter, Geotech Ltd
Shuang Wang, Geotech Ltd
Joseli Soares, Geotech Ltd
Kanita Khaled, Geotech Ltd
Emily Data, Geotech Ltd
Nasreddine Bournas, PhD, PGeo, Geotech Ltd
Jean M. Legault, MSc, PGeo, Geotech Ltd

Date: December, 13th 2019

PROJECT: GOBLIN AND GARGOYLE PROJECT AREAS
LOCATION: ATIKOKAN, ONTARIO
FOR: BALMORAL RESOURCES LTD.
SURVEY FLOWN: NOVEMBER 2018 – APRIL 2019
PROJECT ID: GL180298

Geotech Ltd.
270 Industrial Parkway South
Aurora, ON Canada L4G 3T9

Tel: +1 905 841 5004
Web: www.geotech.ca
Email: info@geotech.ca



TABLE OF CONTENTS

SUMMARY	3
1. INTRODUCTION	5
1.1 Location, Access, Climate and Landscape	6
2. GEOLOGIC SETTING	10
2.1 Regional Geology	10
2.2 Local Geology	10
2.2.1 Gargoyle	10
2.2.2 Goblin	10
3. HISTORIC WORK	12
3.1 Gargoyle	12
3.2 Goblin	12
4. DATA ACQUISITION	14
4.1 Flight path Specifications	14
4.2 Survey Operations	16
4.3 SURVEY SPECIFICATIONS	18
4.4 Aircraft and Equipment	18
4.4.1 Survey Aircraft	18
4.4.2 Electromagnetic System	18
4.4.3 Full waveform vtem™ sensor calibration	22
4.4.4 Horizontal Magnetic Gradiometer	22
4.4.5 Radar Altimeter	22
4.4.6 GPS Navigation System	22
4.4.7 Digital Acquisition System	22
4.5 Base Station	23
5. PERSONNEL	24
6. DATA PROCESSING AND PRESENTATION	25
6.1 Flight Path	25
6.2 Electromagnetic Data	25
6.3 Horizontal Magnetic Gradiometer Data	27
7. DELIVERABLES	28
7.1 Survey Report	28
7.2 Maps	28
7.3 Digital Data	29
8. CONCLUSIONS AND RECOMMENDATIONS	33
9. REFERENCES	35
10. GLOSSARY:	36

LIST OF FIGURES

Figure 1: General Survey location map	6
Figure 2: Survey location map of the Goblin and Gargoyle properties.	7
Figure 3: The Goblin property with claims	8
Figure 4: The Gargoyle property with claims	9
Figure 5: Flight path for the Goblin Block	14
Figure 6: Flight path for the Gargoyle Block	15
Figure 7: VTEM™ Transmitter Current Waveform	19
Figure 8: VTEM™plus System Configuration	21
Figure 9: Z, X and Fraser filtered X (FFx) components for "thin" target	26

LIST OF TABLES

Table 1: Flight path specifications	15
Table 2: Survey schedule	16
Table 3: Off-Time Decay Sampling Scheme	19
Table 4: Acquisition Sampling Rates.....	23
Table 5: Geosoft GDB Data Format	29
Table 6: Geosoft Resistivity Depth Image GDB Data Format	31
Table 7: Geosoft database for the VTEM waveform	32

APPENDICES

A. Survey Location Maps	
B. Survey Survey Area Coordinates	
C. Geophysical Maps	
D. Generalized Modelling Results of the VTEM System.....	
E. TAU Analysis	
F. TEM Resistivity Depth Imaging (RDI).....	
G. Resistivity Depth Images (RDI).....	

SUMMARY

Geotech Ltd carried out a helicopter-borne geophysical survey for the exploration of mineral resources over the Goblin and Gargoyle project areas, located near Atikokan, Ontario, Canada on behalf of Balmoral Resources Ltd. The survey was conducted during the period between November 15th, 2018 and January 11th, 2019 over the Goblin block and between April, 1st 2019 and April 25th 2019 over the Gargoyle block. The geographic coordinates of the centre of the Goblin Block are (Lat 49° 4'37.00"N, Long 91°19'34.01"W) and the geographic coordinates of the centre of the Gargoyle Block are (Lat 49° 3'57.49"N, Long 91° 1'34.41"W).

Principal geophysical sensors included a versatile time domain electromagnetic (VTEM™plus) system and a horizontal magnetic gradiometer with two caesium sensors. Ancillary equipment included a GPS navigation system and a radar altimeter. A total of 2012 line-kilometres of geophysical data were acquired during the survey.

In-field data quality assurance and preliminary processing were carried out on a daily basis during the acquisition phase. Preliminary and final data processing, including generation of final digital data and map products were undertaken from the office of Geotech Ltd. in Aurora, Ontario.

The processed survey results are presented as the following maps:

- Electromagnetic stacked profiles of the B-field Z Component
- Electromagnetic stacked profiles of the dB/dt Z Component
- B-Field Z Component Channel grid image
- Fraser Filtered X Component Channel grid image
- Total Magnetic Intensity (TMI) grid image
- Calculated Time Constant (Tau) grid image with Calculated Vertical Derivative contours
- Resistivity Depth Images (RDI) sections and depth slices

Digital data include all electromagnetic and magnetic products, ancillary data and the EM system waveform.

This survey report describes the procedures for data acquisition, equipment used, processing, final image presentation and the specifications for the digital data set.

Based on the obtained geophysical results, the total magnetic intensity data over the Goblin block shows the presence of a major anomalous zone that occupies most the east side of the block and tapers to the west, extending across the property. A large east-westerly electromagnetic anomaly is found just north of this magnetic feature in the middle of the Goblin block and other narrower, arcuate east-westerly and discontinuous conductive zones just south of it appear to coincide with the magnetic feature and extend across the property.

Over the Gargoyle block, the magnetic data show the presence of three or four major narrow, linear magnetic trends that extend across the block in the WNW-ESE direction. A large circular, intrusive-like magnetic anomaly is also observed in the south-west of Gargoyle block, with a diameter of 3.5km. This anomalous magnetic body is resistive and displaces or truncates the EM conductive trends. The electromagnetic data indicate narrow, slightly discontinuous linear zones of high

conductivity that extend across the center and southern part of the block and either follow or partially coincide with most of the linear magnetic trends with a maximum length of approximately 18 km.

A detailed interpretation and analysis of the VTEM and magnetic dataset are recommended. If the anomalous zones correspond to an exploration model of this area, then it is recommended performing 3D Magnetic Inversion, EM Anomaly Picking and Maxwell Plate modeling of selected EM anomalies. This will help better define the targets prior to drill testing.

1. INTRODUCTION

Geotech Ltd. performed a helicopter-borne geophysical survey over the Goblin and Gargoyle Blocks, Atikokan, Ontario (Figure 1 & Figure 2).

Darin Wagner represented Balmoral Resources Ltd. during the data acquisition and data processing phases of this project.

The geophysical surveys consisted of helicopter borne EM using the versatile time-domain electromagnetic (VTEM™ plus) system with Full-Waveform processing. Measurements consisted of Vertical (Z), in-line Horizontal (X) and cross-line Horizontal (Y) components EM fields using induction coils and the aeromagnetic total field using two caesium magnetometers. A total of 2012 line-km of geophysical data were acquired during the survey.

The crew was based out of Atikokan (Figure 2) in Ontario for the acquisition phase of the survey. Survey flying started November 15th, 2018 to January 11th, 2019 and was completed April 25th, 2019.

Data quality control and quality assurance, and preliminary data processing were carried out on a daily basis during the acquisition phase of the project. Final data processing followed immediately after the end of the survey. Final reporting, data presentation and archiving were completed. A comprehensive interpretation report and additional products were also completed from the Aurora office of Geotech Ltd. in June, 2019.

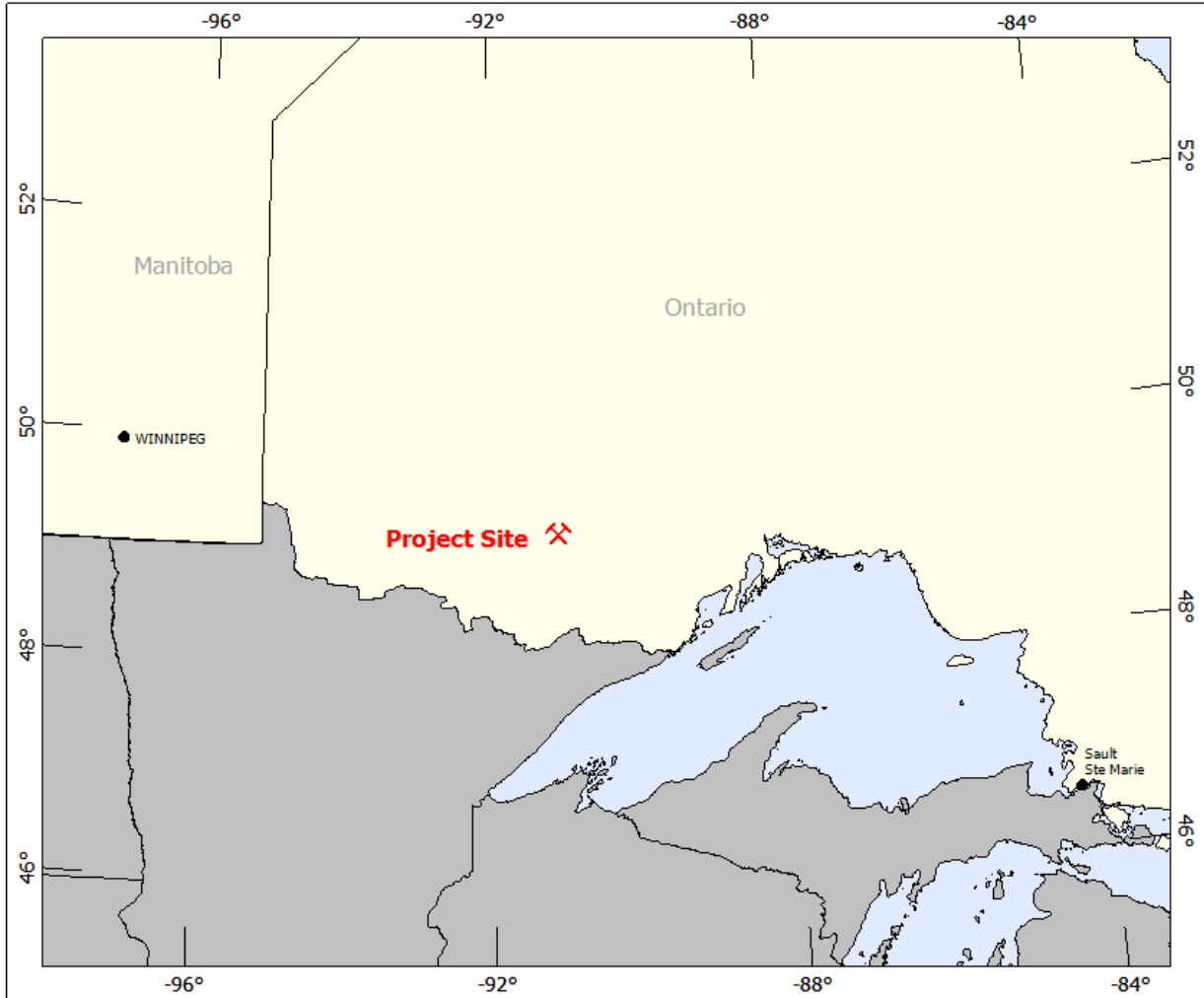


Figure 1: General Survey location map.

1.1 LOCATION, ACCESS, CLIMATE AND LANDSCAPE

The Gargoyle and Goblin properties are located approximately 50 kilometers northeast from the town of Atikokan, Ontario (population 2,800) and 150 kilometers northwest of the city of Thunder Bay, Ontario with population of 110,000, Figure 2.

Hwy 17 is approximately 15 Km to the north while the Trans-Canada Hwy 11 is 40 Km to the south. The properties can be reached by logging roads off Hwy 623, which branches off the Trans-Canada Hwy 11 at the community of Sapawe, ON.

The region experiences cold winters and warm summers with snow cover between November and April. Canadian climate normals from Environment Canada for the nearest weather station in the community of Mine Centre, Ontario indicate that the daily average temperature ranges from -15.4°C in January to 18.6°C in July. The highest average accumulation of rain for a month is 118.7 mm in July. The highest average accumulation of snow for a month is 33.0 cm in December. The highest average snow depth is 39 cm in January (Environment Canada, 2012).

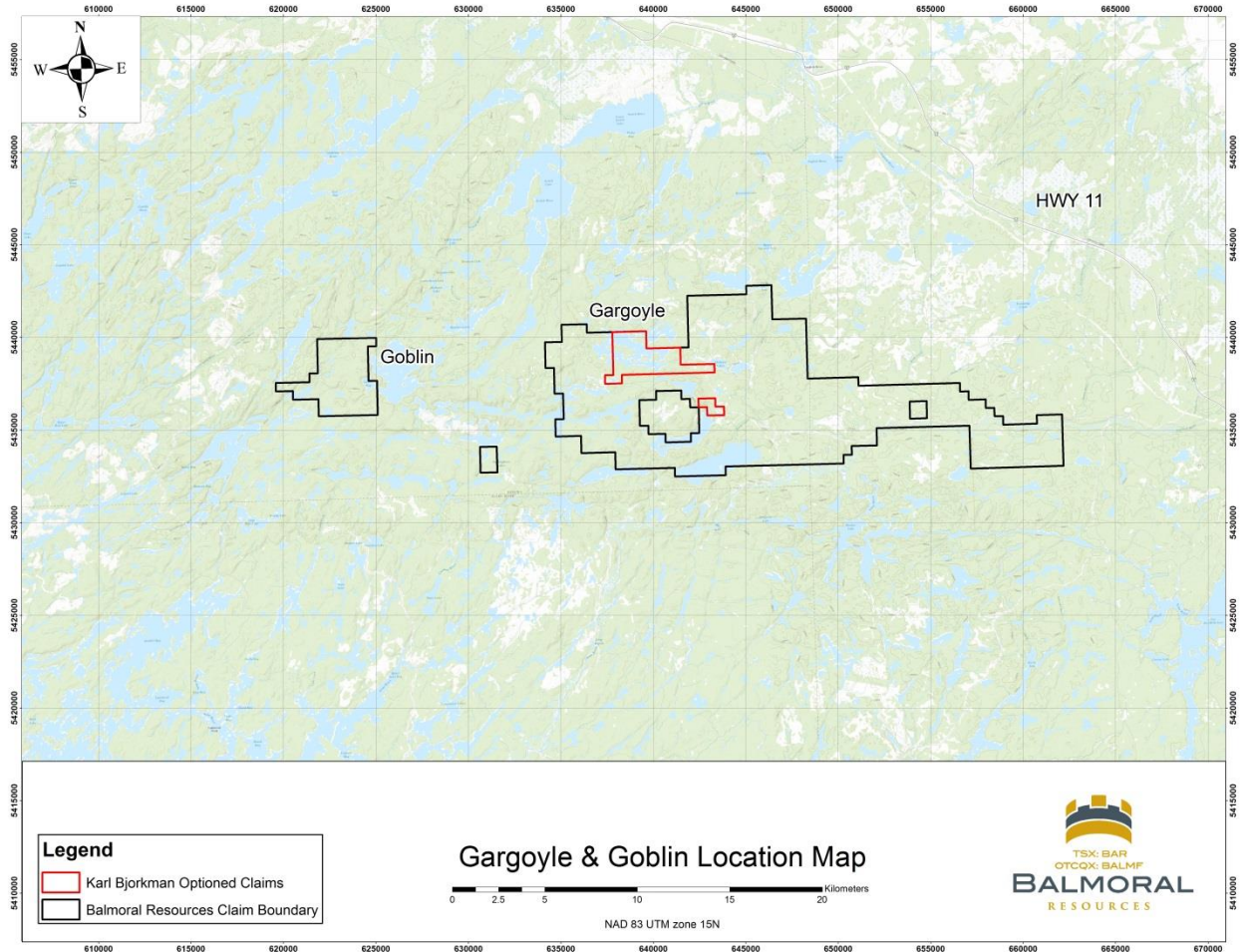


Figure 2: Survey location map of the Goblin and Gargoyle properties.

Figure 3 depicts the Goblin Block boundary with claims and Figure 4 presents the the Gargoyle Block boundary with claims.

The landscape of the area consists of exposed bedrock knobs and ridges with glacial till covering the topographic lows. The till occurs as mainly medium to coarse sand but occasional contains gravel and boulders (Madon, 2010). Lakes up to 4 km long and 1 km wide are present across the property, as well as organic peat, bogs, swamps and marches where topography is low. The overall topography is flat with elevations ranging from 395 to 558 m a.s.l. (Figure 5 and Figure 6).

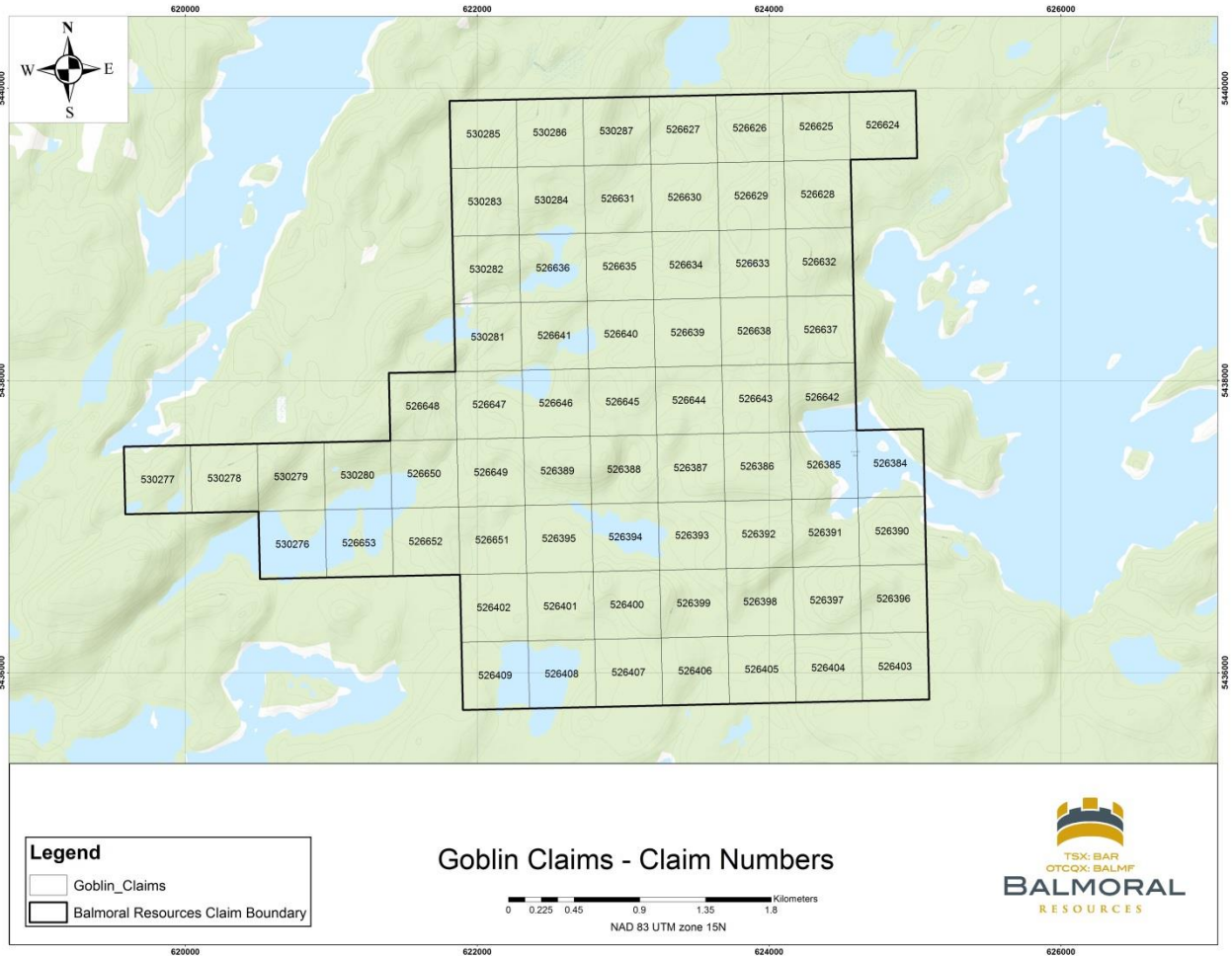


Figure 3: The Goblin property with claims

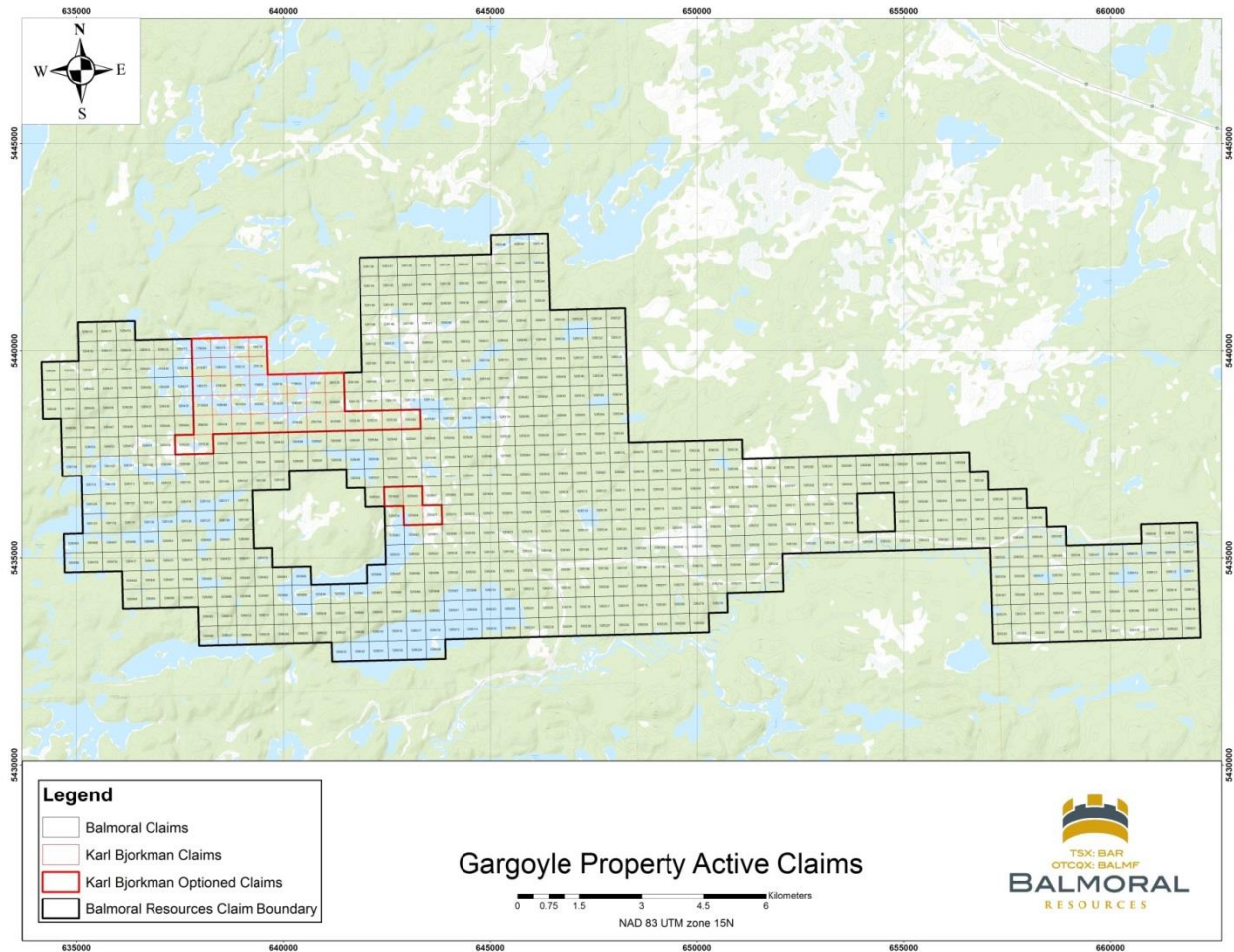


Figure 4: The Gargoyl property with claims

2. GEOLOGIC SETTING

2.1 REGIONAL GEOLOGY

The Gargoyle and Goblin properties lie on the Lumby Lake greenstone belt (3.014 to 2.830 Ga) within the Marmion Terrane of the Wabigoon Subprovince (Tomlinson et al, 1996). The Lumby Lake Greenstone belt is about 60 km long east to west and 20 km wide. It is underlain mainly by mafic to intermediate metavolcanics with minor felsic and komatiitic metavolcanics and metasedimentary rocks. It overlies the Marmion batholith (3003 to 3001 Ma) to the south and occurs at the contact with the Dashwa Lake batholith (2877 Ma) to the northwest by a fault striking in the north-south direction.

The Lumby Lake greenstone belt includes two distinct northern and southern assemblages. The northern assemblage comprises the Lumby North and Pinecone sequences while the southern assemblage comprises the Lumby South and Bar Lake sequences. The rocks of the Lumby Lake greenstone belt are metamorphosed to greenschist facies with occasional upper greenschist to lower amphibolite facies. Chlorite, actinolite, biotite and epidote occur in various amounts within varied metamorphic assemblages.

Historically, mineralization in the Lumby Lake greenstone belt has been found in the southern part of the belt and near the Red Paint Fault zone. Stratabound mineral occurrences and shear-hosted occurrences are the primary types of mineralization. Small amounts of pyrite and pyrrhotite (trace to 2%) are common in the mafic metavolcanic rocks, usually within pillow selvages (Madon, 2010). Between Lumby Lake and Spoon Lake, sheared felsic tuff hosts several stratabound Pb-Zn-Cu-Ag occurrences, which usually include pyrite and occasional pyrrhotite, sphalerite, chalcopyrite, galena and native silver.

2.2 LOCAL GEOLOGY

2.2.1 GARGOYLE

The Gargoyle property lies on the center portion of the Lumby Lake Greenstone belt surrounding the post-tectonic granodioritic Van Nostrand Stock. At the west end of the property, the Bar Lake – Pinecone Shear Zone separates the northern assemblage from the southern assemblage. Based on mapping of the area (Tomlinson et al, 1996), a unit of komatiite flow sequences, separated by argillaceous sulphide-rich iron formations, runs northwest through the property for at least 5 km strike length and is up to 120 m thick in some areas, with individual flows being 4 to 13 m thick. Spinifex texture is common in these komatiites.

2.2.2 GOBLIN

The Goblin property lies on the western end of the Lumby lake property, adjacent to the Red Paint Lake Fault Zone and immediately southwest of the dioritic Norway Lake Pluton. The property consists primarily of mafic and intermediate metavolcanics and metasediments with minor ultramafics. Based on mapping results obtained by Billiton (1984), the property lies on a syncline structure with the hinge striking east to west.

The Gargoyle and Goblin properties contain significant packages of ultramafic rocks (komatiites) that are locally observed to have Ni-Cu-PGE mineralization. It is hypothesized that these komatiite sequences may have basal accumulations of massive sulphides.

A VTEM survey was chosen as a first pass exploration method for two reasons: identify buried komatiitic rocks that are typically associated with strong magnetic features, and map conductive sources at depth that may represent massive Ni-Cu-PGE targets associated with komatiites.

3. HISTORIC WORK

3.1 GARGOYLE

The earliest drilling on the Gargoyle property was in 1954 when Candela Development Co. drilled seventeen holes totalling 1650 meters.

In 1967 Noranda Resources carried out magnetic and VLF-EM surveys between Leo and Hematite Lake and detected conductive and magnetic anomalies. They identified a copper occurrence on the northeast end of Hematite Lake, but no further work was done. They also explored the Firesteel area in the southeast of the property by performing magnetic and EM surveys followed by three diamond drill holes, for which no assays were reported.

In the period between 1968 and 1983, Canadian Nickel Co Ltd. were active on the property, with four drill holes in 1968 and two more in 1983. From 1971 to 1972 they carried out a magnetic survey and drilled two holes south of Mathieu Lake. These holes intersected mafic volcanics and iron formations containing pyrite, pyrrhotite, graphite and magnetite.

In 1971 Canico Resources drilled four holes totalling 397 meters.

In 1974, Falconbridge Nickel Mines Ltd. Drilled 3 holes totalling 155 meters, and reported primarily metavolcanics and metasediments.

From 1982 to 1983, Teck and Cominco carried out ground geophysics and drilling in the Pinecone Lake area.

In 1990, Placer Dome performed ground geophysics 1.5 kilometers south of Gargoyle Lake, which identified several anomalies.

In 1991 Alcanex Ltd completed geological mapping and sampling over the Gargoyle Lake area. Chip sampling across an old trench returned anomalous copper (0.15% over 0.46 m) and zinc (4.3% over 0.15 m). Humus sampling returned anomalous gold of up to 9 ppb (background values <2.4 ppb) as well as Zinc (240 ppm).

From 1994 to 1995 Northstar Soapstone Company Inc. carried out a stripping program on their soapstone deposit located 600 metres northeast of Leo Lake.

From 2009 to 2010 Brett Resources Ltd. were active on Richardson Lake Property (12 claims, 2,385 hectares), which is now the southwest portion of the Gargoyle property. In 2009 they performed prospecting and rock sampling and in 2010 they carried out a regional soil sampling survey over the Richardson Lake Property, which identified some weak and sporadic gold and Cu-Ni anomalies.

3.2 GOBLIN

In 1967 Noranda Exploration performed an electromagnetic survey and detected a broad conductive zone over a zone of highly erratic magnetic anomalies.

In 1984 Billiton Canada Ltd. Carried out a geochemical soil survey over the Red Paint Lake area

which contains the Goblin property.

In 1990, Placer Dome Inc. carried out a total field magnetic survey and a VLF survey west of Norway Lake, which identified forty-two conductors.

4. DATA ACQUISITION

4.1 FLIGHT PATH SPECIFICATIONS

Both properties were flown in a north to south direction (N 0° E / N 180° E) with traverse line spacing of 100 metres as depicted in **Figure 5** and **Figure 6**. Tie lines were flown perpendicular to the traverse lines (N 90° E / N 270° E). For more detailed information on the flight spacing and direction, see Table 1.

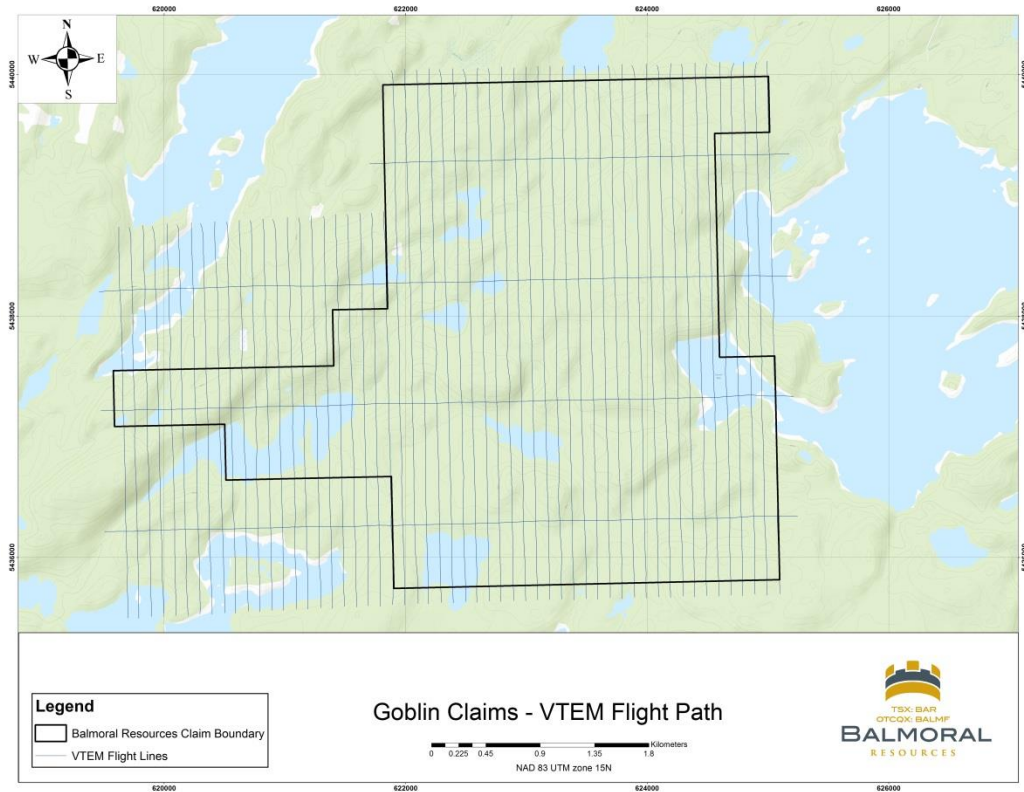


Figure 5: Flight path for the Goblin Block.

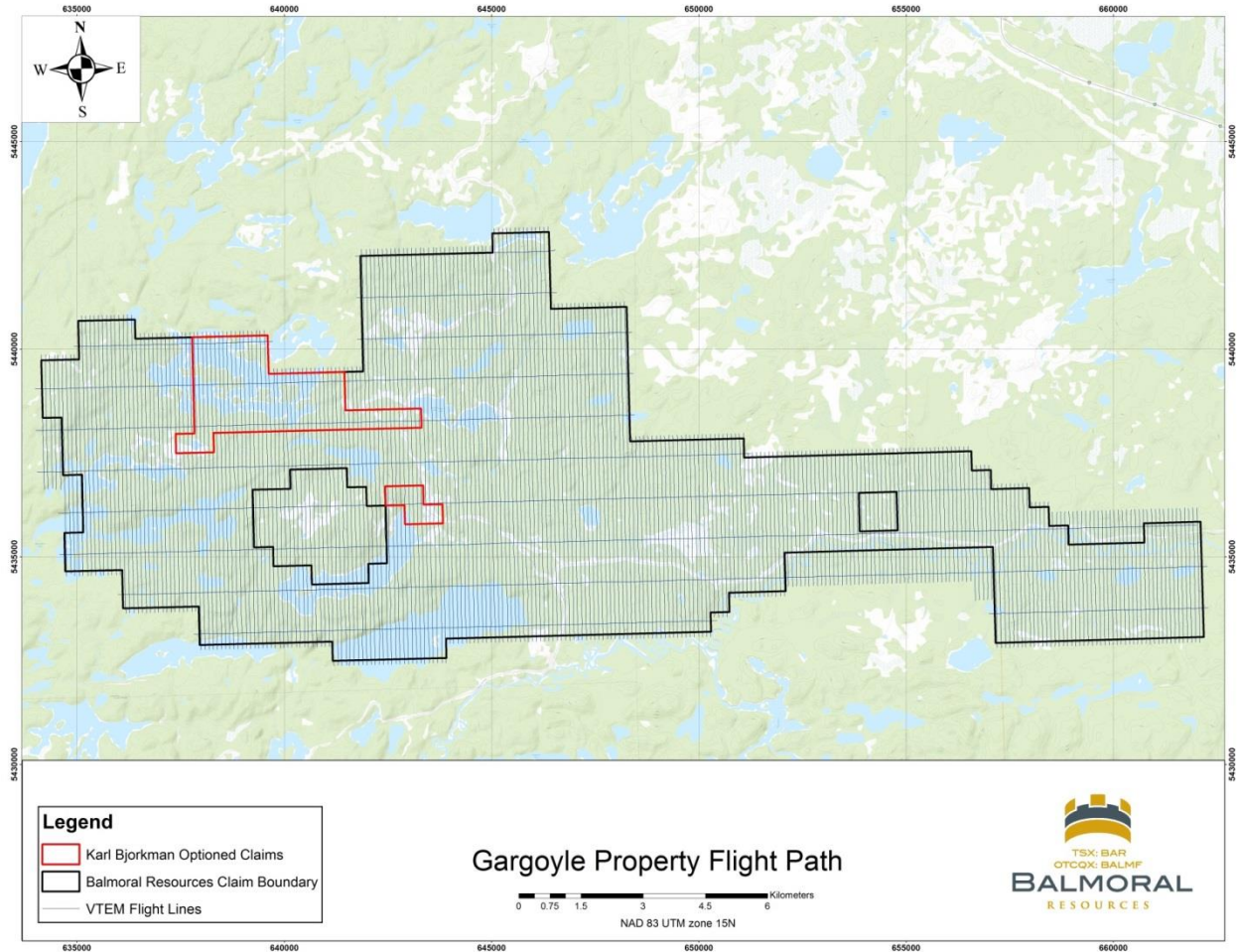


Figure 6: Flight path for the Gargoyle Block.

Table 1: Flight path specifications

Survey block	Line spacing (m)	Area (Km ²)	Planned ¹ Line-km	Actual Line-km	Flight direction	Line numbers
Goblin	Traverse: 100	22	223	237	N 0° E / N 180° E	L1000 – L1540
	Tie: 1000				N 90° E / N 270° E	T2000 – T2030
Gargoyle	Traverse: 100	159	1703	1775	N 0° E / N 180° E	L3000 – L5780
	Tie: 1000				N 90° E / N 270° E	T6000 – T6091
Total		181	1926	2012		

Survey area boundaries co-ordinates are provided in Appendix B.

¹ Note: Actual Line kilometres represent the total line kilometres in the final database. These line-km normally exceed the Planned Line-km, as indicated in the survey NAV files.

4.2 SURVEY OPERATIONS

Survey operations were based out of Atikokan, Ontario. The following table shows the timing of the flying and daily production status.

Table 2: Survey schedule

Date	Comments
15/11/2018	Crew arrived on site.
16/11/2018	System assembly.
17/11/2018	System assembly.
18/11/2018	System assembly.
19/11/2018	System assembly.
20/11/2018	No test flights due to weather.
21/11/2018	System testing.
22/11/2018	No test flights due to weather.
23/11/2018	No test flights due to weather.
24/11/2018	No test flights due to weather.
25/11/2018	System testing.
26/11/2018	No test flights due to weather.
27/11/2018	No test flights due to weather.
28/11/2018	No test flights due to weather.
29/11/2018	No test flights due to weather.
30/11/2018	No test flights due to weather.
01/12/2018	No test flights due to weather.
02/12/2018	No test flights due to weather.
03/12/2018	No test flights due to weather.
04/12/2018	No test flights due to weather.
05/12/2018	No test flights due to weather.
06/12/2018	System testing. System cleared for production.
07/12/2018	Production flight.
08/12/2018	Production flight. 62 km Flown. Flight aborted due to tree strike.
09/12/2018	Loop retrieval.
10/12/2018	Loop retrieval.
11/12/2018	System assembly.
12/12/2018	System assembly.
13/12/2018	System assembly.
15/12/2018	System testing.
16/12/2018	System testing.
17/12/2018	System testing.
18/12/2018	System testing.
19/12/2018	System testing.
20/12/2018	No test flights due to weather.
21/12/2018	Troubleshooting.
22/12/2018	System testing.

Date	Comments
23/12/2018	No production due to weather.
24/12/2018	No production due to weather.
25/12/2018	No production due to weather.
26/12/2018	No production due to weather.
27/12/2018	No production due to weather.
28/12/2018	No production due to weather.
29/12/2018	No production due to weather.
30/12/2018	No production due to weather.
31/12/2018	No production due to weather.
01/01/2019	Production flights completed, 83 km flown.
02/01/2019	Production flight completed, 85 km flown.
03/01/2019	No production due to weather.
04/01/2019	No production due to weather.
05/01/2019	No production due to weather.
06/01/2019	No production due to weather.
07/01/2019	No production due to weather.
08/01/2019	No production due to weather.
09/01/2019	No production due to weather.
10/01/2019	No production possible due to weather. Crew commenced demobilization. Survey postponed until April.
01/04/2019	Crew arrived in Atikokan.
02/04/2019	System assembly.
03/04/2019	System assembly.
04/04/2019	System assembly.
05/04/2019	System assembly.
06/04/2019	System testing.
07/04/2019	System testing.
08/04/2019	System testing.
09/04/2019	No test flights due to weather.
10/04/2019	System testing.
11/04/2019	Production flight aborted due to weather. 14km flown.
12/04/2019	No production due to weather.
13/04/2019	No production due to weather.
14/04/2019	4 production flights completed, 388km flown.
15/04/2019	2 production flights completed, 256km flown.
16/04/2019	3 production flights completed, 257km flown.
17/04/2019	No production due to weather.
18/04/2019	No production due to weather.
19/04/2019	3 production flights completed, 298km flown.
20/04/2019	No production due to weather.
21/04/2019	3 production flights completed, 242km flown.
22/04/2019	2 production flights completed, 199km flown.
23/04/2019	1 production flight completed, 22km flown. Flight path completed.

Date	Comments
24/04/2019	System disassembly and demobilization.
25/04/2019	System disassembly and demobilization. Crew departed Atikotan.

4.3 SURVEY SPECIFICATIONS

During the survey the helicopter was maintained at a mean altitude of 99 metres above the ground with an average survey speed of 89 km/hour. This allowed for an actual average EM transmitter-receiver loop terrain clearance of 64 metres and a magnetic sensor clearance of 74 metres.

The on board operator was responsible for monitoring the system integrity. He also maintained a detailed flight log during the survey, tracking the times of the flight as well as any unusual geophysical or topographic features.

On return of the aircrew to the base camp the survey data was transferred from a compact flash card (PCMCIA) to the data processing computer. The data were then uploaded via ftp to the Geotech office in Aurora for daily quality assurance and quality control by qualified personnel.

4.4 AIRCRAFT AND EQUIPMENT

4.4.1 SURVEY AIRCRAFT

The survey was flown using a Eurocopter Aerospatiale (A-star) 350 B3 helicopter, registration C-GVMU. The helicopter is owned and operated by Geotech Aviation. Installation of the geophysical and ancillary equipment was carried out by a Geotech Ltd crew.

4.4.2 ELECTROMAGNETIC SYSTEM

The electromagnetic system was a Geotech Time Domain EM (VTEM™plus) full receiver-waveform streamed data recorded system. The “full waveform VTEM system” uses the streamed half-cycle recording of transmitter and receiver waveforms to obtain a complete system response calibration throughout the entire survey flight. VTEM with the Serial number 32 had been used for the survey. The VTEM™ transmitter current waveform is shown diagrammatically in Figure 7.

The VTEM™ Receiver and transmitter coils were in concentric-coplanar and Z-direction oriented configuration. The receiver system for the project also included a coincident-coaxial X-direction coil to measure the in-line dB/dt and the B-Field responses. The Transmitter-receiver loop was towed at a mean distance of 34 metres below the aircraft as shown in Figure 8.

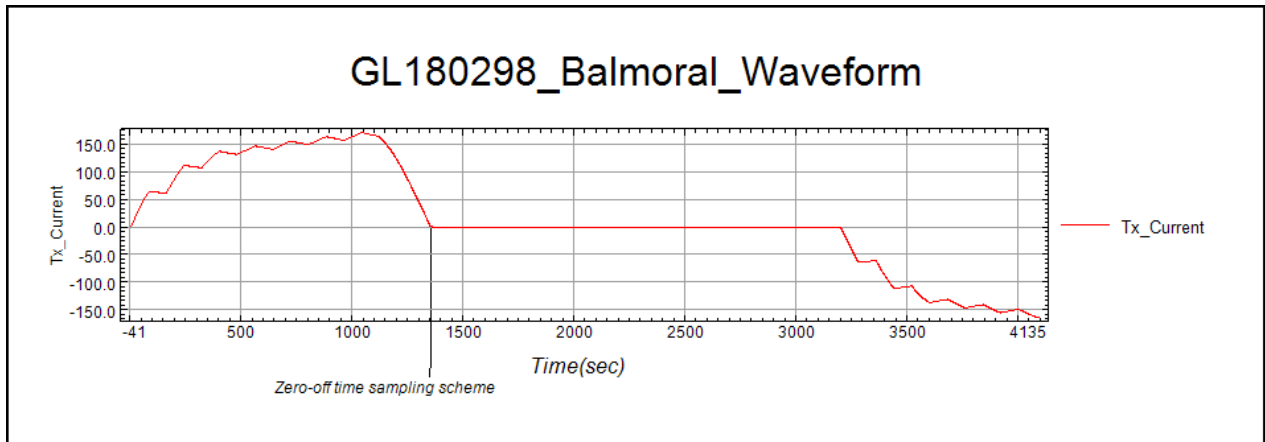


Figure 7: VTEM™ Transmitter Current Waveform

The VTEM™ decay sampling scheme is shown in Table 3 below. Forty-three time measurement gates were used for the final data processing in the range from 0.021 to 8.083 msec. Zero time for the off-time sampling scheme is equal to the current pulse width and is defined as the time near the end of the turn-off ramp where the dI/dt waveform falls to 1/2 of its peak value.

Table 3: Off-Time Decay Sampling Scheme

VTEM™ Decay Sampling Scheme				
Index	Start	End	Middle	Width
Milliseconds				
4	0.018	0.023	0.021	0.005
5	0.023	0.029	0.026	0.005
6	0.029	0.034	0.031	0.005
7	0.034	0.039	0.036	0.005
8	0.039	0.045	0.042	0.006
9	0.045	0.051	0.048	0.007
10	0.051	0.059	0.055	0.008
11	0.059	0.068	0.063	0.009
12	0.068	0.078	0.073	0.010
13	0.078	0.090	0.083	0.012
14	0.090	0.103	0.096	0.013
15	0.103	0.118	0.110	0.015
16	0.118	0.136	0.126	0.018
17	0.136	0.156	0.145	0.020
18	0.156	0.179	0.167	0.023
19	0.179	0.206	0.192	0.027
20	0.206	0.236	0.220	0.030
21	0.236	0.271	0.253	0.035
22	0.271	0.312	0.290	0.040

VTEM™ Decay Sampling Scheme				
Index	Start	End	Middle	Width
Milliseconds				
23	0.312	0.358	0.333	0.046
24	0.358	0.411	0.383	0.053
25	0.411	0.472	0.440	0.061
26	0.472	0.543	0.505	0.070
27	0.543	0.623	0.580	0.081
28	0.623	0.716	0.667	0.093
29	0.716	0.823	0.766	0.107
30	0.823	0.945	0.880	0.122
31	0.945	1.086	1.010	0.141
32	1.086	1.247	1.161	0.161
33	1.247	1.432	1.333	0.185
34	1.432	1.646	1.531	0.214
35	1.646	1.891	1.760	0.245
36	1.891	2.172	2.021	0.281
37	2.172	2.495	2.323	0.323
38	2.495	2.865	2.667	0.370
39	2.865	3.292	3.063	0.427
40	3.292	3.781	3.521	0.490
41	3.781	4.341	4.042	0.560
42	4.341	4.987	4.641	0.646
43	4.987	5.729	5.333	0.742
44	5.729	6.581	6.125	0.852
45	6.581	7.560	7.036	0.979
46	7.560	8.685	8.083	1.125

Z Component: 4 - 46 time gates

X Component: 20 - 46 time gates

Y Component: 20 - 46 time gates

VTEM™ system specifications:

Transmitter	Receiver
<ul style="list-style-type: none"> • Transmitter loop diameter: 26 m • Number of turns: 4 • Effective Transmitter loop area: 2123.7 m² • Transmitter base frequency: 30 Hz • Peak current: 170.5 A • Pulse width: 7.06 ms • Waveform shape: Bi-polar trapezoid • Peak dipole moment: 364,884 nIA • Average transmitter-receiver loop terrain clearance: 64 metres 	<ul style="list-style-type: none"> • X Coil diameter: 0.32 m • Number of turns: 245 • Effective coil area: 19.69 m² • Y Coil diameter: 0.32 m • Number of turns: 245 • Effective coil area: 19.69 m² • Z-Coil diameter: 1.2 m • Number of turns: 100 • Effective coil area: 113.04 m²

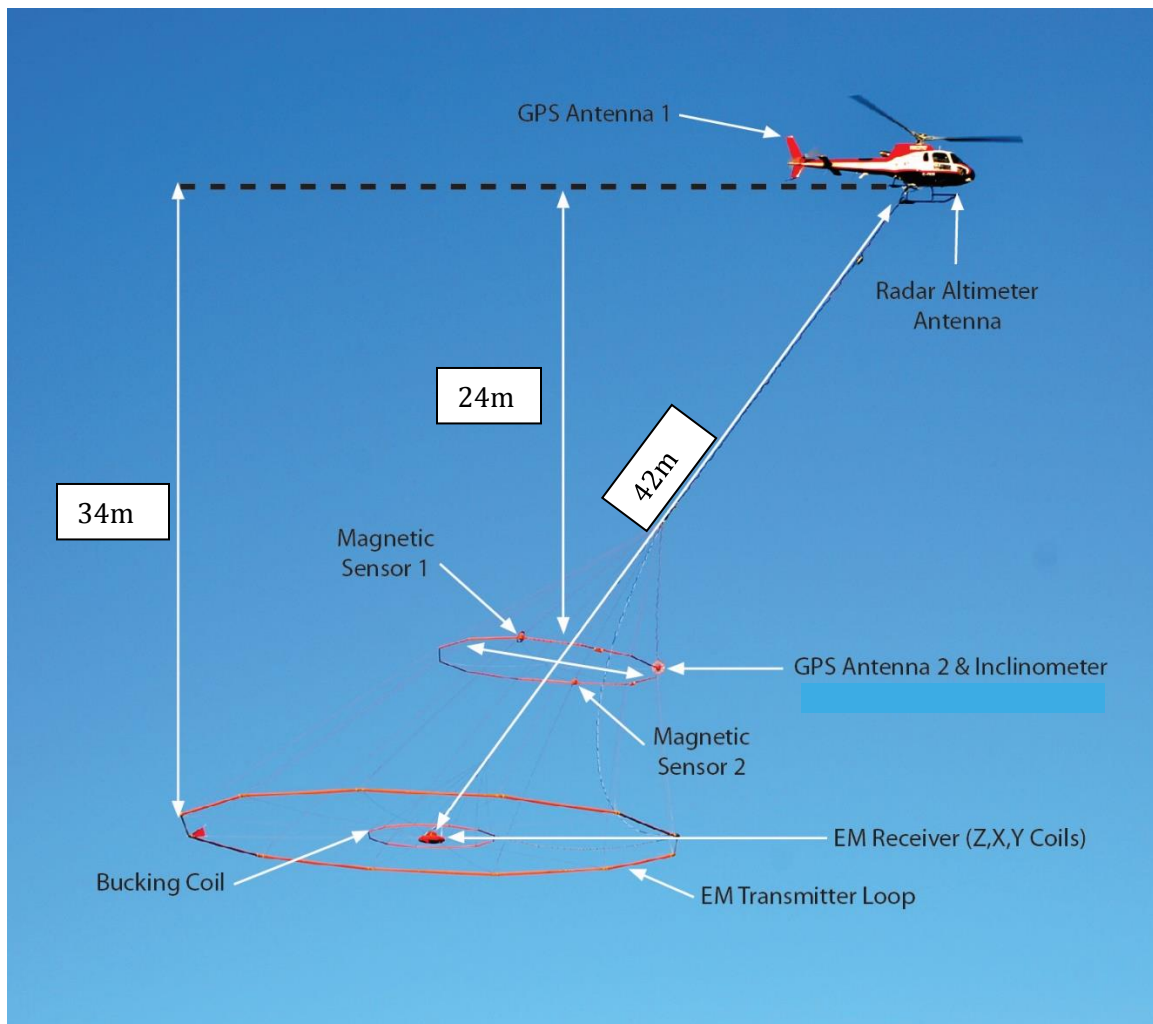


Figure 8: VTEM™plus System Configuration.

4.4.3 FULL WAVEFORM VTEM™ SENSOR CALIBRATION

The calibration is performed on the complete VTEM™ system installed in and connected to the helicopter, using special calibration equipment. This calibration takes place on the ground at the start of the project prior to surveying.

The procedure takes half-cycle files acquired and calculates a calibration file consisting of a single stacked half-cycle waveform. The purpose of the stacking is to attenuate natural and man-made magnetic signals, leaving only the response to the calibration signal.

This calibration allows the transfer function between the EM receiver and data acquisition system and also the transfer function of the current monitor and data acquisition system to be determined. These calibration results are then used in VTEM full waveform processing.

4.4.4 HORIZONTAL MAGNETIC GRADIOMETER

The horizontal magnetic gradiometer consists of two Geometrics split-beam field magnetic sensors with a sampling interval of 0.1 seconds. These sensors are mounted 12.5 metres apart on a separate loop, 10 metres above the Transmitter-receiver loop. A GPS antenna and Gyro Inclinator is installed on the separate loop to accurately record the tilt and position of the magnetic gradiometer.

4.4.5 RADAR ALTIMETER

A Terra TRA 3000/TRI 40 radar altimeter was used to record terrain clearance. The antenna was mounted beneath the bubble of the helicopter cockpit (Figure 8).

4.4.6 GPS NAVIGATION SYSTEM

The navigation system used was a Geotech PC104 based navigation system utilizing a NovAtel's WAAS (Wide Area Augmentation System) enabled GPS receiver, Geotech navigate software, a full screen display with controls in front of the pilot to direct the flight and a NovAtel GPS antenna mounted on the helicopter tail (Figure 8). As many as 11 GPS and two WAAS satellites may be monitored at any one time. The positional accuracy or circular error probability (CEP) is 1.8 m, with WAAS active, it is 1.0 m. The co-ordinates of the survey area were set-up prior to the survey and the information was fed into the airborne navigation system. The second GPS antenna is installed on the additional magnetic loop together with Gyro Inclinator.

4.4.7 DIGITAL ACQUISITION SYSTEM

A Geotech data acquisition system recorded the digital survey data on an internal compact flash card. Data is displayed on an LCD screen as traces to allow the operator to monitor the integrity of the system. The data type and sampling interval as provided in Table 4

Table 4: Acquisition Sampling Rates

Data Type	Sampling
TDEM	0.1 sec
Magnetometer	0.1 sec
GPS Position	0.2 sec
Radar Altimeter	0.2 sec
Inclinometer	0.1 sec

4.5 BASE STATION

A combined magnetometer/GPS base station was utilized on this project. A Geometrics Caesium vapour magnetometer was used as a magnetic sensor with a sensitivity of 0.001 nT. The base station was recording the magnetic field together with the GPS time at 1 Hz on a base station computer.

The base station magnetometer sensor was installed in a secured location away from electric transmission lines and moving ferrous objects such as motor vehicles. The base station data were backed-up to the data processing computer at the end of each survey day.

5. PERSONNEL

The following Geotech Ltd. personnel were involved in the project.

FIELD:

Project Manager:	Shauna-Lee Hewett (Office)
Data QC:	Nick Venter
Crew chief:	Christian Oertel
Operator:	Mduduzi Maphumulo

The survey pilot and the mechanical engineer were employed directly by the helicopter operator – HeliCarrier Helicopters.

Pilot:	Jocelyn Vallieres
Mechanical Engineer:	Charles Picard

OFFICE:

Preliminary Data Processing:	Nick Venter
Final Data Processing:	Shuang Wang
Data QA/QC:	Kanita Khaled, P. Geo and Emily Data
Reporting/Mapping:	Joseli Soares and Nasreddine Bournas, PhD, P.Geo

Processing and reporting phases were carried out under the supervision of Emily Data, Data Processing Manager. The customer relations were looked after by David Hitz.

6. DATA PROCESSING AND PRESENTATION

Data compilation and processing were carried out by the application of Geosoft OASIS Montaj and programs proprietary to Geotech Ltd.

6.1 FLIGHT PATH

The flight path, recorded by the acquisition program as WGS 84 latitude/longitude, was converted into the NAD83 Datum, UTM Zone 15N coordinate system in Oasis Montaj.

The flight path was drawn using linear interpolation between x and y positions from the navigation system. Positions are updated every second and expressed as UTM easting's (x) and UTM northing's (y).

6.2 ELECTROMAGNETIC DATA

The Full Waveform EM specific data processing operations included:

- Half cycle stacking (performed at time of acquisition);
- System response correction;
- Parasitic and drift removal.

A three stage digital filtering process was used to reject major spheric events and to reduce noise levels. Local spheric activity can produce sharp, large amplitude events that cannot be removed by conventional filtering procedures. Smoothing or stacking will reduce their amplitude but leave a broader residual response that can be confused with geological phenomena. To avoid this possibility, a computer algorithm searches out and rejects the major spheric events.

The signal to noise ratio was further improved by the application of a low pass linear digital filter. This filter has zero phase shift which prevents any lag or peak displacement from occurring, and it suppresses only variations with a wavelength less than about 1 second or 15 metres. This filter is a symmetrical 1 sec linear filter.

The results are presented as stacked profiles of EM voltages for the time gates, in linear - logarithmic scale for the B-field Z component and dB/dt responses in the Z and X components. B-field Z component time channels recorded at 0.440 milliseconds after the termination of the impulse is also presented as a colour image. Calculated Time Constant (TAU) with Calculated Vertical Derivative contours is presented in Appendix C. Resistivity Depth Image (RDI) is also presented in Appendix F and G.

VTEM™ has three receiver coil orientations. Z-axis coil is oriented parallel to the transmitter coil axis and both are horizontal to the ground. The X-axis coil is oriented parallel to the ground and along the line-of-flight. The Y-axis coil is oriented parallel to the ground and perpendicular to the line-of-flight. This combined three coil configuration provides information on the position, depth, dip and thickness of a conductor. Generalized modeling results of VTEM data, are shown in Appendix D.

In general X-component data produce cross-over type anomalies: from “+ to -” in flight direction of flight for “thin” sub vertical targets and from “- to +” in direction of flight for “thick” targets. Z component data produce double peak type anomalies for “thin” sub vertical targets and single peak for “thick” targets.

The limits and change-over of “thin-thick” depends on dimensions of a TEM system (Appendix D, Figure D-16).

Because of X component polarity is under line-of-flight, convolution Fraser Filter (Figure 9) is applied to X component data to represent axes of conductors in the form of grid map. In this case positive FF anomalies always correspond to “plus-to-minus” X data crossovers independent of the flight direction.

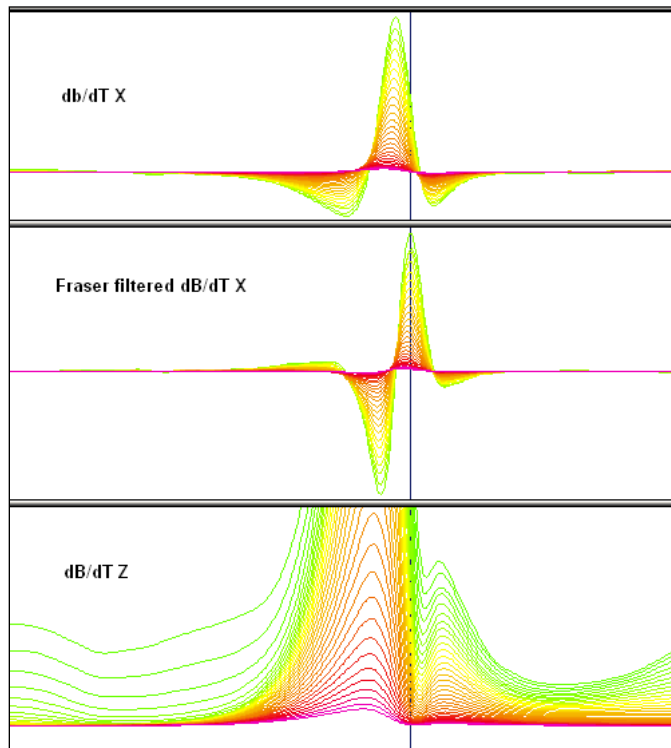


Figure 9: Z, X and Fraser filtered X (FFx) components for “thin” target.

6.3 HORIZONTAL MAGNETIC GRADIOMETER DATA

The horizontal gradients data from the VTEM™Plus are measured by two magnetometers 12.5 m apart on an independent bird mounted 10m above the VTEM™ loop. A GPS and a Gyro Inclinator help to determine the positions and orientations of the magnetometers. The data from the two magnetometers are corrected for position and orientation variations, as well as for the diurnal variations using the base station data.

The position of the centre of the horizontal magnetic gradiometer bird is calculated from the GPS utilizing in-house processing tool in Geosoft. Following that total magnetic intensity is calculated at the center of the bird by calculating the mean values from both sensors. In addition to the total intensity advanced processing is done to calculate the in-line and cross-line (or lateral) horizontal gradient which enhance the understanding of magnetic targets. The in-line (longitudinal) horizontal gradient is calculated from the difference of two consecutive total magnetic field readings divided by the distance along the flight line direction, while the cross-line (lateral) horizontal magnetic gradient is calculated from the difference in the magnetic readings from both magnetic sensors divided by their horizontal separation.

Two advanced magnetic derivative products, the total horizontal derivative (THDR), and tilt angle derivative and are also created. The total horizontal derivative or gradient is defined as:

$THDR = \sqrt{H_x^2 + H_y^2}$, where H_x and H_y are cross-line and in-line horizontal gradients.

The tilt angle derivative (TDR) is defined as:

$TDR = \arctan(V_z / THDR)$, where THDR is the total horizontal derivative, and V_z is the vertical derivative.

Measured cross-line gradients can help to enhance cross-line linear features during gridding.

7. DELIVERABLES

7.1 SURVEY REPORT

The survey report describes the data acquisition, processing, and final presentation of the survey results. The survey report is provided in two paper copies and digitally in PDF format.

7.2 MAPS

Final maps were produced at scale of 1:20,000 for best representation of the survey size and line spacing. The coordinate/projection system used was NAD83 Datum, UTM Zone 15N. All maps show the flight path trace and topographic data; latitude and longitude are also noted on maps.

The preliminary and final results of the survey are presented as EM profiles, a late-time gate gridded EM channel, and a colour magnetic TMI contour map.

- Maps at 1:15,000 in Geosoft MAP format, as follows:

GL180298_15k_dBdt:	dB/dt profiles Z Component, Time Gates 0.220 – 7.036 ms in linear – logarithmic scale.
GL180298_15k_BField:	B-field profiles Z Component, Time Gates 0.220 – 7.036 ms in linear – logarithmic scale.
GL180298_15k_BFz25:	B-field Z Component Channel 25, Time Gate 0.440 ms colour image.
GL180298_15k_SFz25:	VTEM dB/dt Z Component Channel 25, Time Gate 0.440 ms.
GL180298_15k_SFxFF30:	Fraser Filtered dB/dt X Component Channel 30, Time Gate 0.880 ms colour image.
GL180298_15k_TMI:	Total Magnetic Intensity (TMI) colour image and contours.
GL180298_15k_TauSF:	dB/dt Calculated Time Constant (Tau) with Calculated Vertical Derivative contours

- Maps are also presented in PDF format.
- The topographic data base was derived from 1:50,000 CANVEC data
- A Google Earth file *GL180298_Balmoral.kmz* showing the flight path of the block is included. Free versions of Google Earth software from: <http://earth.google.com/download-earth.html>

7.3 DIGITAL DATA

Two copies of the data and maps on DVD were prepared to accompany the report. Each DVD contains a digital file of the line data in GDB Geosoft Montaj format as well as the maps in Geosoft Montaj Map and PDF format.

- DVD structure.

Data contains databases, grids and maps, as described below.
 Report contains a copy of the report and appendices in PDF format.

Databases in Geosoft GDB format, containing the channels listed in Table 5.

Table 5: Geosoft GDB Data Format

Channel name	Units	Description
X:	metres	Easting NAD83 Zone 15N
Y:	metres	Northing NAD83 Zone 15N
Longitude:	Decimal Degrees	WGS84 Longitude data
Latitude:	Decimal Degrees	WGS84 Latitude data
Z:	metres	GPS antenna elevation (above Geoid)
Zb:	metres	EM bird elevation (above Geoid)
Radar:	metres	helicopter terrain clearance from radar altimeter
Radarb:	metres	Calculated EM transmitter-receiver loop terrain clearance from radar altimeter
DEM:	metres	Digital Elevation Model
Gtime:	Seconds of the day	GPS time
Mag1L:	nT	Measured Total Magnetic field data (left sensor)
Mag1R:	nT	Measured Total Magnetic field data (right sensor)
Basemag:	nT	Magnetic diurnal variation data
Mag2LZ	nT	Z corrected (w.r.t. loop center) and diurnal corrected magnetic field left mag
Mag2RZ	nT	Z corrected (w.r.t. loop center) and diurnal corrected magnetic field right mag
TMI2	nT	Calculated from diurnal corrected total magnetic field intensity of the centre of the loop
TMI3	nT	Microleveled total magnetic field intensity of the centre of the loop
Hginline		Calculated in-line gradient
Hgcxline		Measured cross-line gradient
CVG	nT/m	Calculated Magnetic Vertical Gradient
SFz[4]:	pV/(A*m ⁴)	Z dB/dt 0.021 millisecond time channel
SFz[5]:	pV/(A*m ⁴)	Z dB/dt 0.026 millisecond time channel
SFz[6]:	pV/(A*m ⁴)	Z dB/dt 0.031 millisecond time channel
SFz[7]:	pV/(A*m ⁴)	Z dB/dt 0.036 millisecond time channel
SFz[8]:	pV/(A*m ⁴)	Z dB/dt 0.042 millisecond time channel
SFz[9]:	pV/(A*m ⁴)	Z dB/dt 0.048 millisecond time channel
SFz[10]:	pV/(A*m ⁴)	Z dB/dt 0.055 millisecond time channel

Channel name	Units	Description
SFz[11]:	pV/(A*m ⁴)	Z dB/dt 0.063 millisecond time channel
SFz[12]:	pV/(A*m ⁴)	Z dB/dt 0.073 millisecond time channel
SFz[13]:	pV/(A*m ⁴)	Z dB/dt 0.083 millisecond time channel
SFz[14]:	pV/(A*m ⁴)	Z dB/dt 0.096 millisecond time channel
SFz[15]:	pV/(A*m ⁴)	Z dB/dt 0.110 millisecond time channel
SFz[16]:	pV/(A*m ⁴)	Z dB/dt 0.126 millisecond time channel
SFz[17]:	pV/(A*m ⁴)	Z dB/dt 0.145 millisecond time channel
SFz[18]:	pV/(A*m ⁴)	Z dB/dt 0.167 millisecond time channel
SFz[19]:	pV/(A*m ⁴)	Z dB/dt 0.192 millisecond time channel
SFz[20]:	pV/(A*m ⁴)	Z dB/dt 0.220 millisecond time channel
SFz[21]:	pV/(A*m ⁴)	Z dB/dt 0.253 millisecond time channel
SFz[22]:	pV/(A*m ⁴)	Z dB/dt 0.290 millisecond time channel
SFz[23]:	pV/(A*m ⁴)	Z dB/dt 0.333 millisecond time channel
SFz[24]:	pV/(A*m ⁴)	Z dB/dt 0.383 millisecond time channel
SFz[25]:	pV/(A*m ⁴)	Z dB/dt 0.440 millisecond time channel
SFz[26]:	pV/(A*m ⁴)	Z dB/dt 0.505 millisecond time channel
SFz[27]:	pV/(A*m ⁴)	Z dB/dt 0.580 millisecond time channel
SFz[28]:	pV/(A*m ⁴)	Z dB/dt 0.667 millisecond time channel
SFz[29]:	pV/(A*m ⁴)	Z dB/dt 0.766 millisecond time channel
SFz[30]:	pV/(A*m ⁴)	Z dB/dt 0.880 millisecond time channel
SFz[31]:	pV/(A*m ⁴)	Z dB/dt 1.010 millisecond time channel
SFz[32]:	pV/(A*m ⁴)	Z dB/dt 1.161 millisecond time channel
SFz[33]:	pV/(A*m ⁴)	Z dB/dt 1.333 millisecond time channel
SFz[34]:	pV/(A*m ⁴)	Z dB/dt 1.531 millisecond time channel
SFz[35]:	pV/(A*m ⁴)	Z dB/dt 1.760 millisecond time channel
SFz[36]:	pV/(A*m ⁴)	Z dB/dt 2.021 millisecond time channel
SFz[37]:	pV/(A*m ⁴)	Z dB/dt 2.323 millisecond time channel
SFz[38]:	pV/(A*m ⁴)	Z dB/dt 2.667 millisecond time channel
SFz[39]:	pV/(A*m ⁴)	Z dB/dt 3.063 millisecond time channel
SFz[40]:	pV/(A*m ⁴)	Z dB/dt 3.521 millisecond time channel
SFz[41]:	pV/(A*m ⁴)	Z dB/dt 4.042 millisecond time channel
SFz[42]:	pV/(A*m ⁴)	Z dB/dt 4.641 millisecond time channel
SFz[43]:	pV/(A*m ⁴)	Z dB/dt 5.333 millisecond time channel
SFz[44]:	pV/(A*m ⁴)	Z dB/dt 6.125 millisecond time channel
SFz[45]:	pV/(A*m ⁴)	Z dB/dt 7.036 millisecond time channel
SFz[46]:	pV/(A*m ⁴)	Z dB/dt 8.083 millisecond time channel
SFx[20]:	pV/(A*m ⁴)	X dB/dt 0.220 millisecond time channel
SFx[21]:	pV/(A*m ⁴)	X dB/dt 0.253 millisecond time channel
SFx[22]:	pV/(A*m ⁴)	X dB/dt 0.290 millisecond time channel
SFx[23]:	pV/(A*m ⁴)	X dB/dt 0.333 millisecond time channel
SFx[24]:	pV/(A*m ⁴)	X dB/dt 0.383 millisecond time channel
SFx[25]:	pV/(A*m ⁴)	X dB/dt 0.440 millisecond time channel
SFx[26]:	pV/(A*m ⁴)	X dB/dt 0.505 millisecond time channel
SFx[27]:	pV/(A*m ⁴)	X dB/dt 0.580 millisecond time channel
SFx[28]:	pV/(A*m ⁴)	X dB/dt 0.667 millisecond time channel
SFx[29]:	pV/(A*m ⁴)	X dB/dt 0.766 millisecond time channel
SFx[30]:	pV/(A*m ⁴)	X dB/dt 0.880 millisecond time channel
SFx[31]:	pV/(A*m ⁴)	X dB/dt 1.010 millisecond time channel

Channel name	Units	Description
SFx[32]:	$\text{pV}/(\text{A}\cdot\text{m}^4)$	X dB/dt 1.161 millisecond time channel
SFx[33]:	$\text{pV}/(\text{A}\cdot\text{m}^4)$	X dB/dt 1.333 millisecond time channel
SFx[34]:	$\text{pV}/(\text{A}\cdot\text{m}^4)$	X dB/dt 1.531 millisecond time channel
SFx[35]:	$\text{pV}/(\text{A}\cdot\text{m}^4)$	X dB/dt 1.760 millisecond time channel
SFx[36]:	$\text{pV}/(\text{A}\cdot\text{m}^4)$	X dB/dt 2.021 millisecond time channel
SFx[37]:	$\text{pV}/(\text{A}\cdot\text{m}^4)$	X dB/dt 2.323 millisecond time channel
SFx[38]:	$\text{pV}/(\text{A}\cdot\text{m}^4)$	X dB/dt 2.667 millisecond time channel
SFx[39]:	$\text{pV}/(\text{A}\cdot\text{m}^4)$	X dB/dt 3.063 millisecond time channel
SFx[40]:	$\text{pV}/(\text{A}\cdot\text{m}^4)$	X dB/dt 3.521 millisecond time channel
SFx[41]:	$\text{pV}/(\text{A}\cdot\text{m}^4)$	X dB/dt 4.042 millisecond time channel
SFx[42]:	$\text{pV}/(\text{A}\cdot\text{m}^4)$	X dB/dt 4.641 millisecond time channel
SFx[43]:	$\text{pV}/(\text{A}\cdot\text{m}^4)$	X dB/dt 5.333 millisecond time channel
SFx[44]:	$\text{pV}/(\text{A}\cdot\text{m}^4)$	X dB/dt 6.125 millisecond time channel
SFx[45]:	$\text{pV}/(\text{A}\cdot\text{m}^4)$	X dB/dt 7.036 millisecond time channel
SFx[46]:	$\text{pV}/(\text{A}\cdot\text{m}^4)$	X dB/dt 8.083 millisecond time channel
BFz	$(\text{pV}\cdot\text{ms})/(\text{A}\cdot\text{m}^4)$	Z B-Field data for time channels 4 to 46
BFX	$(\text{pV}\cdot\text{ms})/(\text{A}\cdot\text{m}^4)$	X B-Field data for time channels 20 to 46
SFxFF	$\text{pV}/(\text{A}\cdot\text{m}^4)$	Fraser Filtered X dB/dt
SFy	$\text{pV}/(\text{A}\cdot\text{m}^4)$	Y dB/dt data for time channels 20 to 46
BFy	$(\text{pV}\cdot\text{ms})/(\text{A}\cdot\text{m}^4)$	Y B-Field data for time channels 20 to 46
NchanBF		Latest time channels of TAU calculation
TauBF	ms	Time constant B-Field
NchanSF		Latest time channels of TAU calculation
TauSF	ms	Time constant dB/dt
PLM:		60 Hz power line monitor

Electromagnetic B-field and dB/dt Z component data is found in array channel format between indexes 4 – 46 and X component data from 20 – 46

- Database of the Resistivity Depth Images in Geosoft GDB format, containing the following channels:

Table 6: Geosoft Resistivity Depth Image GDB Data Format

Channel name	Units	Description
Xg	metres	Easting NAD83 Zone 15N
Yg	metres	Northing NAD83 Zone 15N
Dist:	meters	Distance from the beginning of the line
Depth:	meters	array channel, depth from the surface
Z:	meters	array channel, depth from sea level
AppRes:	Ohm-m	array channel, Apparent Resistivity
TR:	meters	EM system height from sea level
Topo:	meters	digital elevation model
Radarb:	metres	Calculated EM transmitter-receiver loop terrain clearance from radar altimeter
SF:	$\text{pV}/(\text{A}\cdot\text{m}^4)$	array channel, dB/dT
MAG:	nT	TMI data
CVG:	nT/m	CVG data
DOI:	metres	Depth of Investigation: a measure of VTEM depth effectiveness

Channel name	Units	Description
PLM:		60Hz Power Line Monitor

- Database of the VTEM Waveform “GL180298_Waveform.gdb” in Geosoft GDB format, containing the following channels:

Table 7: Geosoft database for the VTEM waveform

Channel name	Units	Description
Time:	milliseconds	Sampling rate interval, 5.2083 microseconds
Tx_Current:	amps	Output current of the transmitter

- Geosoft Resistivity Depth Image Products:

Sections: Apparent resistivity sections along each line in .GRD and .PDF format
Slices: Apparent resistivity slices at selected depths from 25m to depth of investigation, at an increment of 25m in .GRD and .PDF format
Voxel: 3D Voxel imaging of apparent resistivity data clipped by digital elevation and depth of investigation

- Grids in Geosoft GRD and GeoTIFF format, as follows:

GL180298_BFz25:	B-Field Z Component Channel 25 (Time Gate 0.440ms)
GL180298_CVG:	Calculated Vertical Derivative (nT/m)
GL180298_DEM:	Digital Elevation Model (m)
GL180298_Hgcxline:	Measured Cross-Line Gradient (nT/m)
GL180298_Hginline:	Measured In-Line Gradient (nT/m)
GL180298_SFxFF25:	Fraser Filtered dB/dt X Component Channel 25 (Time Gate 0.440 ms)
GL180298_TauBF:	B-Field Z Component, Calculated Time Constant (ms)
GL180298_TauSF:	dB/dt Z Component, Calculated Time Constant (ms)
GL180298_TMI:	Total Magnetic Intensity (nT)
GL180298_PLM:	60Hz Power Line Monitor
GL180298_SFz8:	dB/dt Z Component Channel 8 (Time Gate 0.042 ms)
GL180298_SFz25:	dB/dt Z Component Channel 25 (Time Gate 0.440 ms)
GL180298_SFz40:	dB/dt Z Component Channel 40 (Time Gate 3.521ms)

A Geosoft .GRD file has a .GI metadata file associated with it, containing grid projection information. A grid cell size of 25 metres was used.

8. CONCLUSIONS AND RECOMMENDATIONS

A helicopter-borne versatile time domain electromagnetic (VTEM™plus), horizontal magnetic gradiometer geophysical survey has been completed over Goblin and Gargoyle Projects, Atikokan, Ontario.

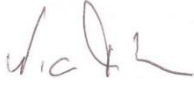
The total area coverage is 181 km². Total survey line coverage is 2012 line kilometres. The principal sensors included a Time Domain EM system, horizontal magnetic gradiometer using two caesium magnetometers system. Results have been presented as stacked profiles, and contour colour images at a scale of 1:15,000. A formal Interpretation has not been included or requested.

Based on the obtained geophysical results, the total magnetic intensity data over the Goblin block shows the presence of a major anomalous zone that occupies most the east side of the block and tapers to the west, extending across the property. A large east-westerly electromagnetic anomaly is found just north of this magnetic feature in the middle of the Goblin block and other narrower, arcuate east-westerly and discontinuous conductive zones just south of it appear to coincide with the magnetic feature and extend across the property.

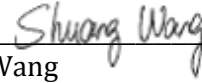
Over the Gargoyle block, the magnetic data show the presence of three or four major narrow, linear magnetic trends that extend across the block in the WNW-ESE direction. A large circular, intrusive-like magnetic anomaly is also observed in the south-west of Gargoyle block, with a diameter of 3.5km. This anomalous magnetic body is resistive and displaces or truncates the EM conductive trends. The electromagnetic data indicate narrow, slightly discontinuous linear zones of high conductivity that extend across the center and southern part of the block and either follow or partially coincide with most of the linear magnetic trends with a maximum length of approximately 18 km.

A detailed interpretation and analysis of the VTEM and magnetic dataset are recommended. If the anomalous zones correspond to an exploration model of this area, then it is recommended performing 3D Magnetic Inversion, EM Anomaly Picking and Maxwell Plate modeling of selected EM anomalies. This will help better define the targets prior to drill testing.

Respectfully submitted².



Nick Venter
Geotech Ltd.



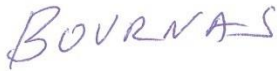
Shuang Wang
Geotech Ltd.



Kanita Khaled, P.Ge
Geotech Ltd.



Joseli Soares
Geotech Ltd.



Nasreddine Bournas, PhD, P.Ge
Geotech Ltd.



Emily Data
Geotech Ltd.



Jean M. Legault, MSc, P.Ge
Geotech Ltd.

December, 2019.

² Final data processing of the EM and magnetic data were carried out by Shuang Wang, from the office of Geotech Ltd. in Aurora, Ontario, under the supervision of Kanita Khaled, P. Geo.

9. REFERENCES

Environment Canada, 2012, National Climate Data and Information Archive, URL
<http://www.climate.weatheroffice.gc.ca/climate_normals/index_e.html>.

Tomlinson, K. Y., Hughs, D.J., Thurston, P.C., 1996, Metavolcanic Rocks of the Central Wabigoon Subprovince: 1) The Lumby Lake Greenstone Belt, 17. Project Unit 95-27, Summary of Field Work and Other Activities.

Madon, Z., 2010, Report on Exploration Activities on the Richardson Lake Property, Thunder Bay Mining Division, Northwestern Ontario, Brett Resources Inc.

Bernatchez, R.A., 1992, A Report on the Lumby Lake Area.

Bernatchez, R.A., 1995, Leo Lake Soapstone Deposit 1994-95 Stripping Program, Northstar Soapstone Company Inc.

Robertson, D., 1984, Report on Geochemical Surveys, Red Paint Lake Property, Project 924, Norway Lake & Richardson Lake Areas Kenora District, Ontario, Billiton Canada Ltd.

Troup W. R., 1991, The Richardson Lake Project, Alcanex Ltd.

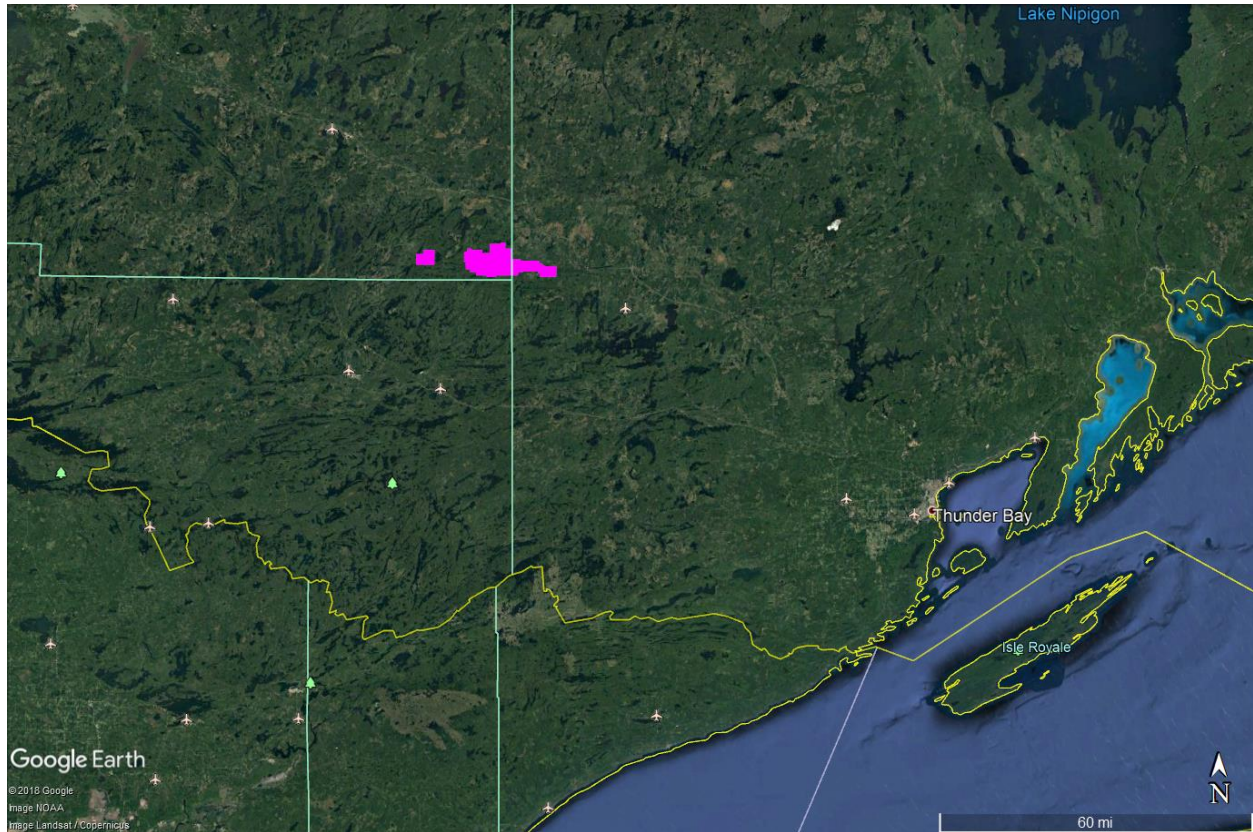
Racic, L., 1990, Magnetic and VLF-Electromagnetic Surveys, Project 392, Norway Lake Area, Ontario, Placer Dome Inc.

10. GLOSSARY:

VTEM – Versatile Time domain ElectroMagnetic
GPS : Global Positioning System
TMI : Total Magnetic Intensity
Tau : Time Constant
B-Field : Electromagnetic Induction Field
dB/dt : Time derivative of the Electromagnetic Induction Field
RDI : Resistivity Depth Imaging
di/dt : Time derivative of the Transmitter Current
NIA – Product of Number of turns, Current and Area of the Transmitter
A : Ampere
Ms : millisecond
M : Metres
KM : Kiliometres
EM : ElectroMagnetic
WASS : Wide Area Augmentation System
UTM : Universal Transverse Mercator
CEP : Circular Error Probability
LCD : Liquid Crystal Display
TDEM : Time Domain ElectroMagnetics
QC : Quality Control
QA : Quality Assurance
THDR : Total Horizontal Derivative
TDR : Tilt Angle Derivative
NAD83 : North America Datum, 1983
WGS-84: World Geodetic System, 1984
Hginline : Inline Horizontal Gradient
Hgcxline : Cross line Horizontal Gradient
PLM: Power Line Monitor

APPENDIX A

SURVEY AREA LOCATION MAP



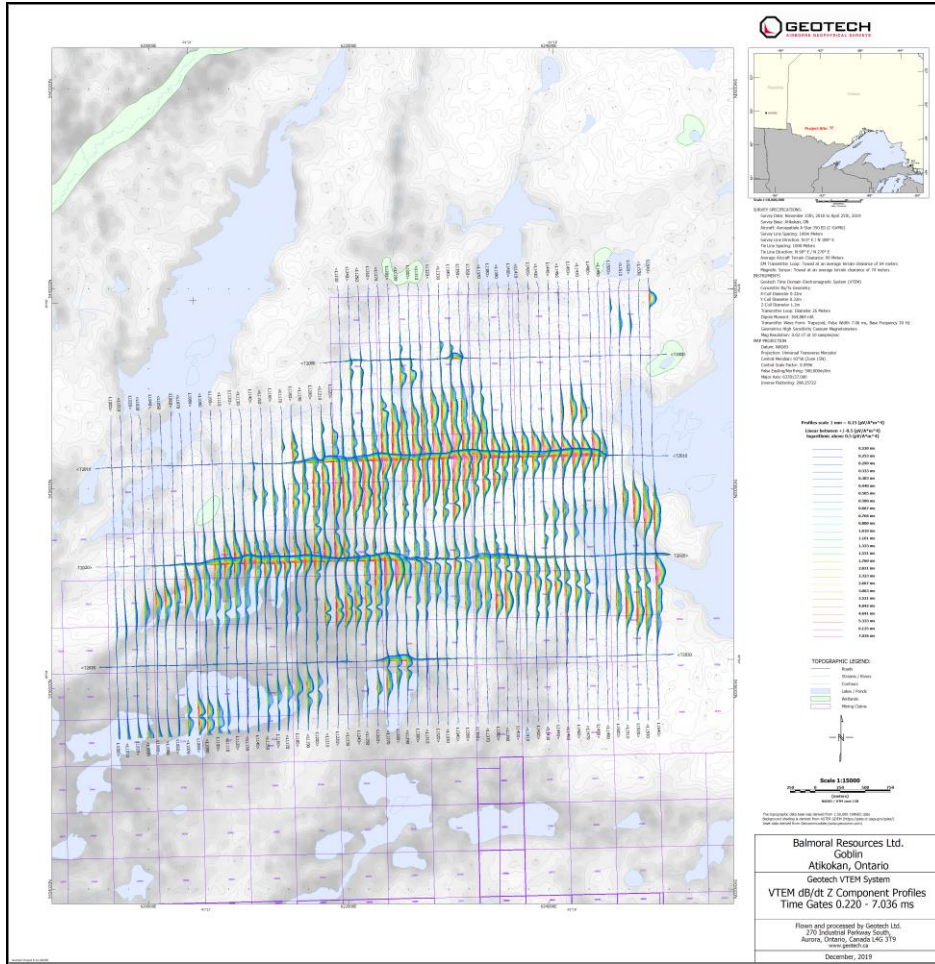
Overview of the Survey Area on a Google Earth image

APPENDIX B

SURVEY AREA COORDINATES (NAD83 UTM 15N)

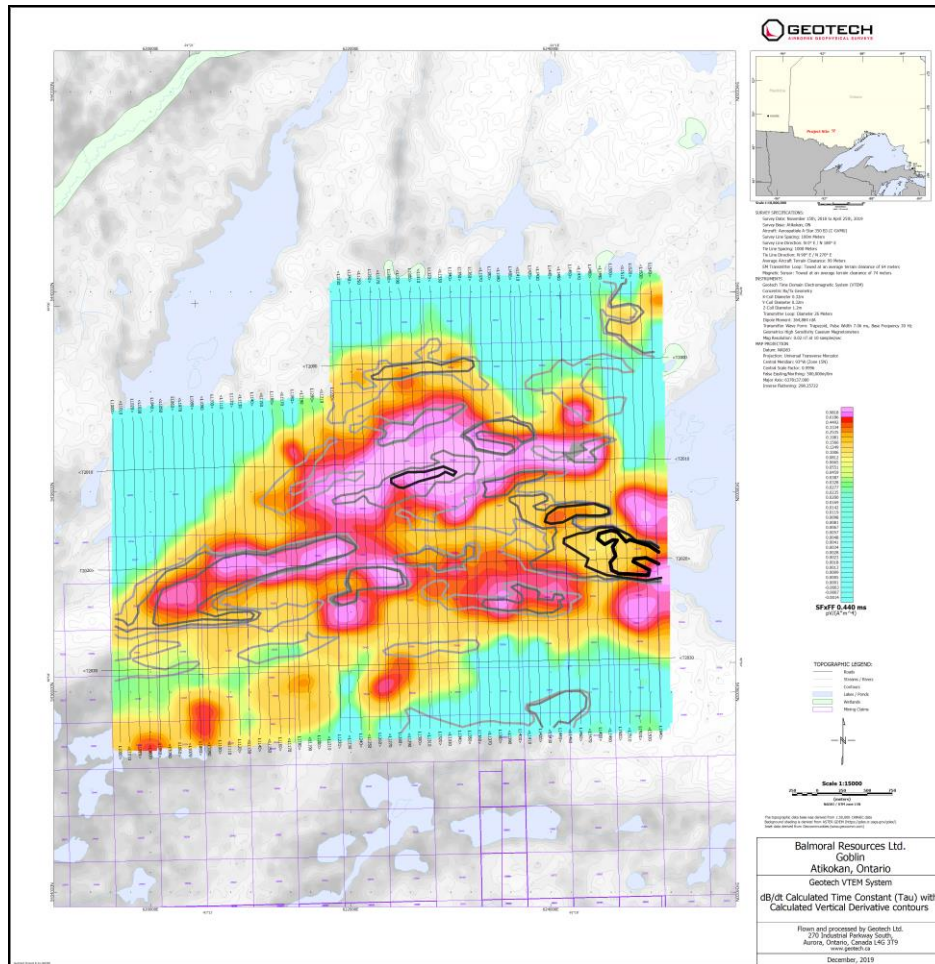
Goblin		Gargoyle			
X, m	Y, m	X, m	Y, m	X, m	Y, m
621901	621901	637961	5432877	648343	5437780
621881	621881	637938	5433804	651082	5437854
620512	620512	636111	5433759	651094	5437391
620502	620502	636088	5434685	656572	5437544
619589	619589	634718	5434651	656585	5437080
619579	619579	634696	5435578	657041	5437093
621404	621404	635152	5435589	657054	5436630
621394	621394	635118	5436978	657967	5436656
621850	621850	634662	5436967	657981	5436193
621810	621810	634628	5438357	658437	5436206
625003	625003	634172	5438346	658450	5435743
625013	625013	634138	5439735	658907	5435756
624557	624557	635051	5439757	658920	5435293
624599	624599	635028	5440684	660747	5435345
625055	625055	636396	5440717	660733	5435809
625097	625097	636408	5440254	662103	5435849
		639601	5440334	662184	5433078
		639625	5439407	657159	5432925
		641906	5439465	657094	5435241
		641835	5442244	652071	5435101
		645027	5442327	652096	5434174
		645015	5442790	650726	5434137
		646382	5442826	650739	5433674
		646432	5440974	650282	5433661
		648256	5441022	650294	5433198

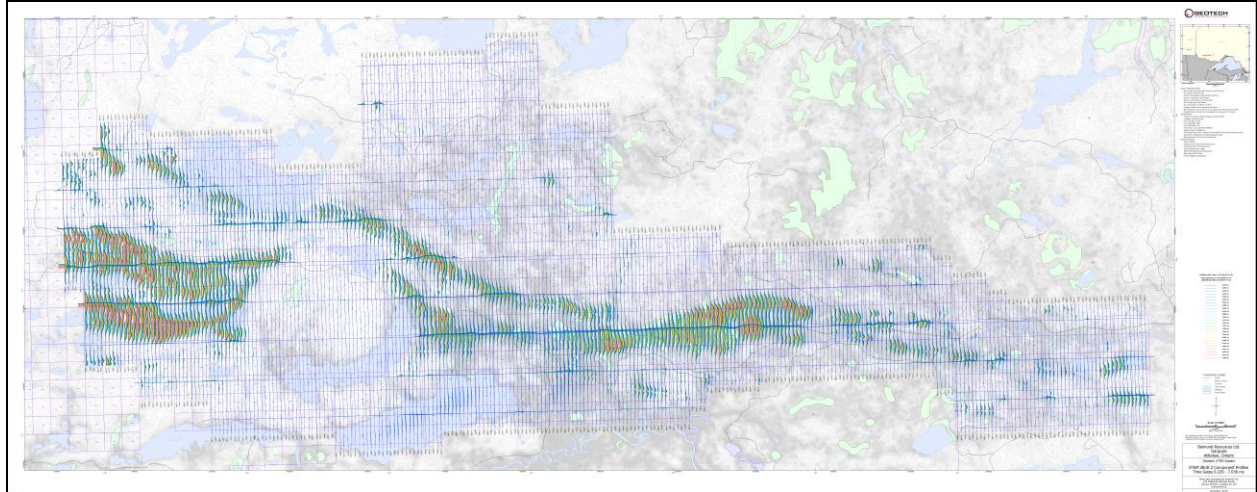
APPENDIX C - GEOPHYSICAL MAPS¹



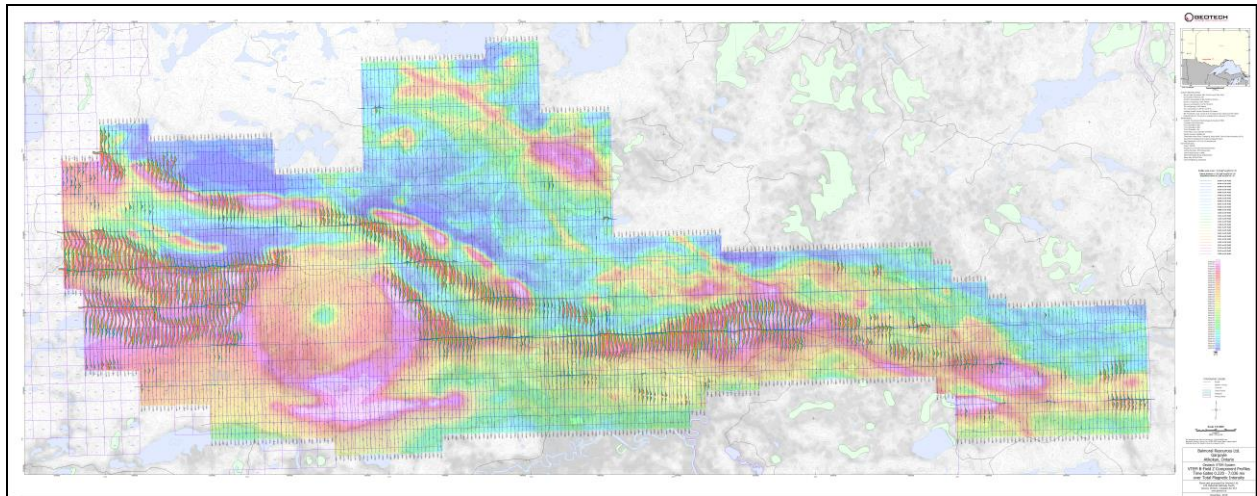
dB/dt profiles Z Component, Time Gates 0.220 – 7.036 ms in linear - Goblin

¹ Complete full size geophysical maps are also available in PDF format located in the final data maps folder

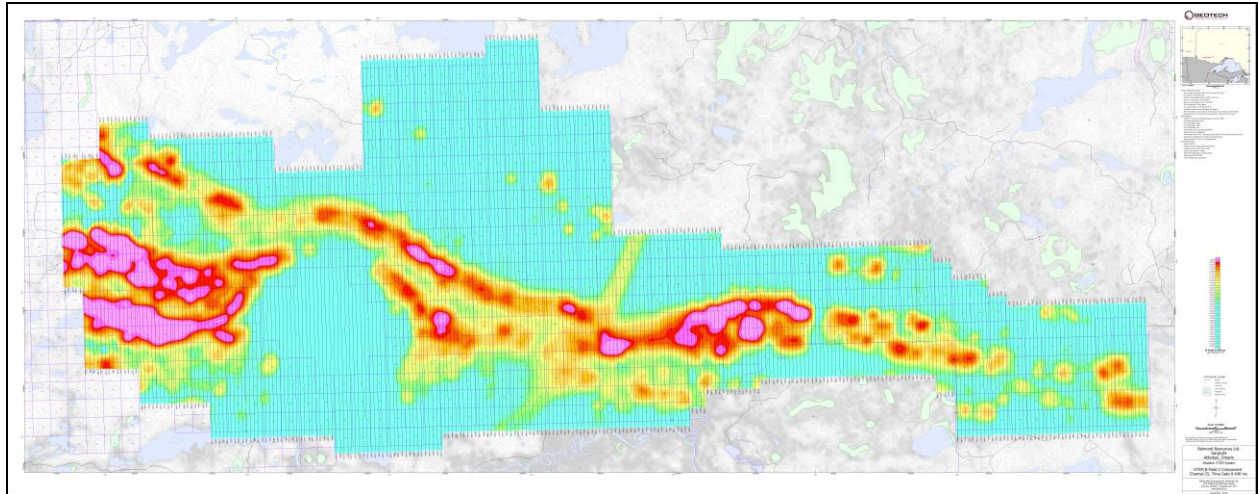




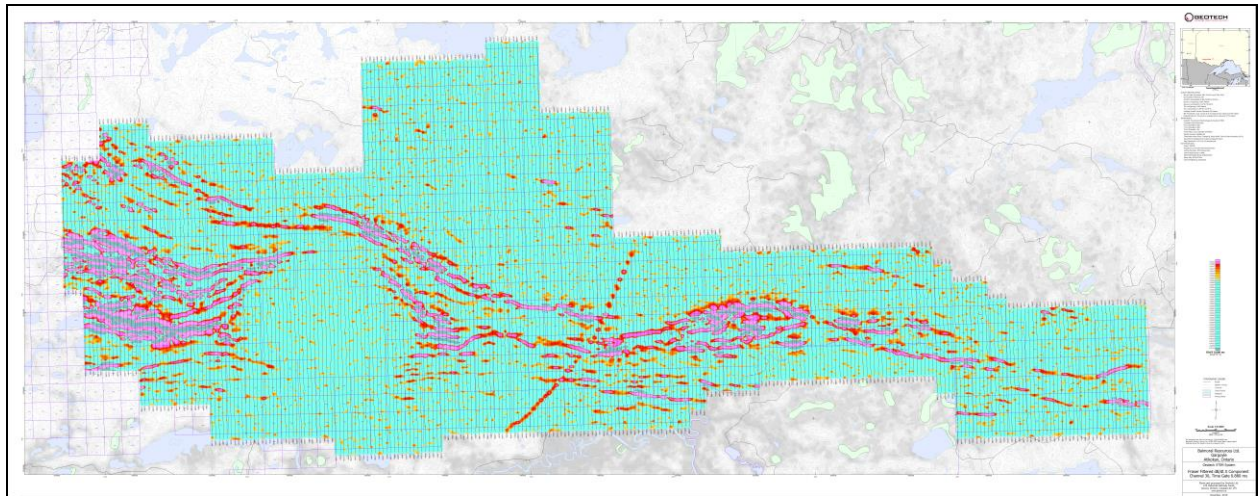
dB/dt profiles Z Component, Time Gates 0.220 – 7.036 ms in linear - Gargoyle



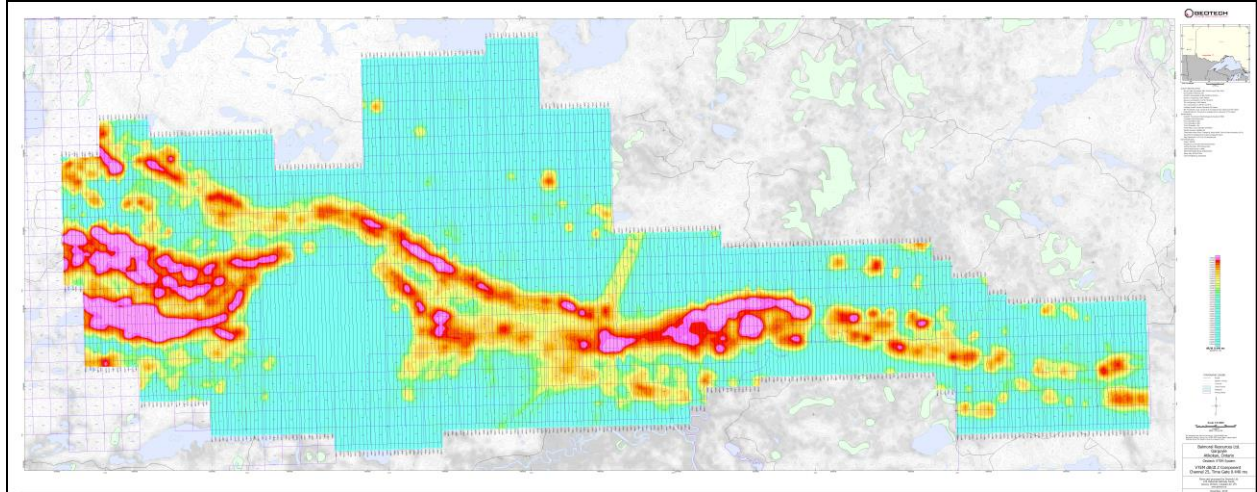
B-field profiles Z Component, Time Gates 0.220 – 7.036 ms in linear - Gargoyle



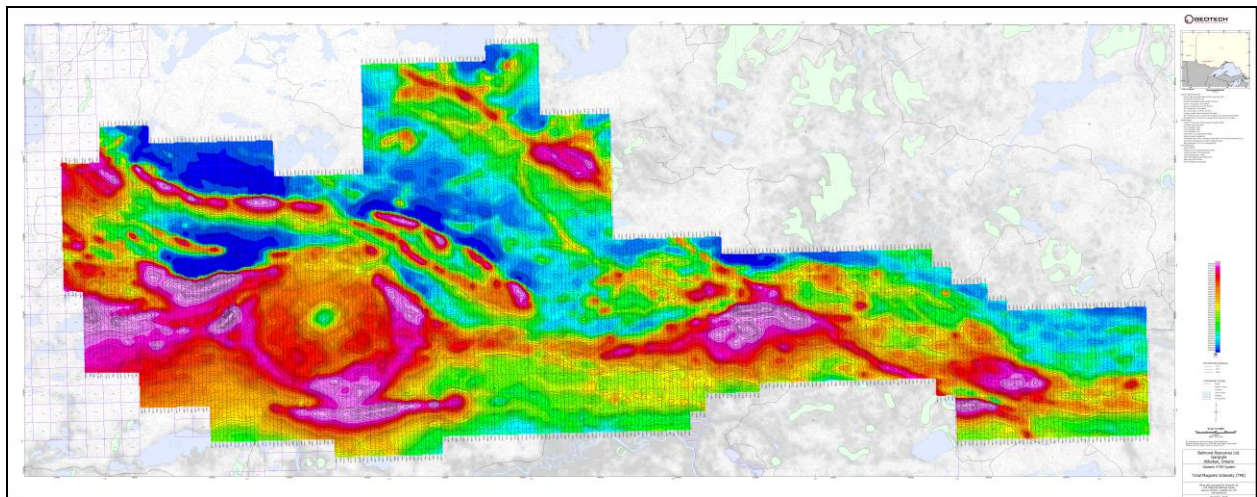
B-field Z Component Channel 25, Time Gate 0.440 ms - Gargoyle



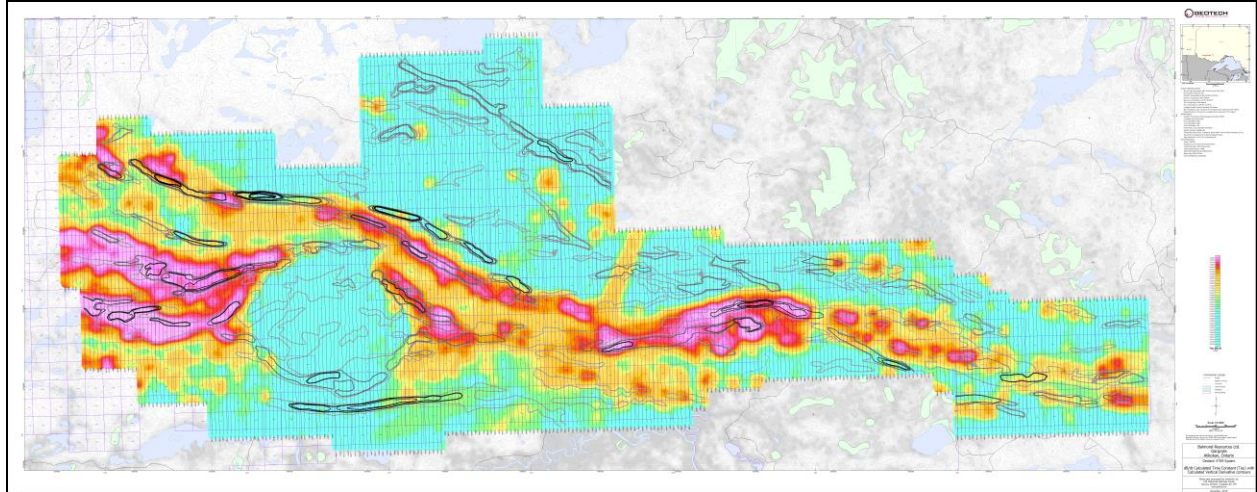
Fraser Filtered dB/dt X Component Channel 30 (Time Gate 0.880 ms) - Gargoyle



VTEM dB/dt Z Component Channel 25, Time Gate 0.440 ms - Gargoyle



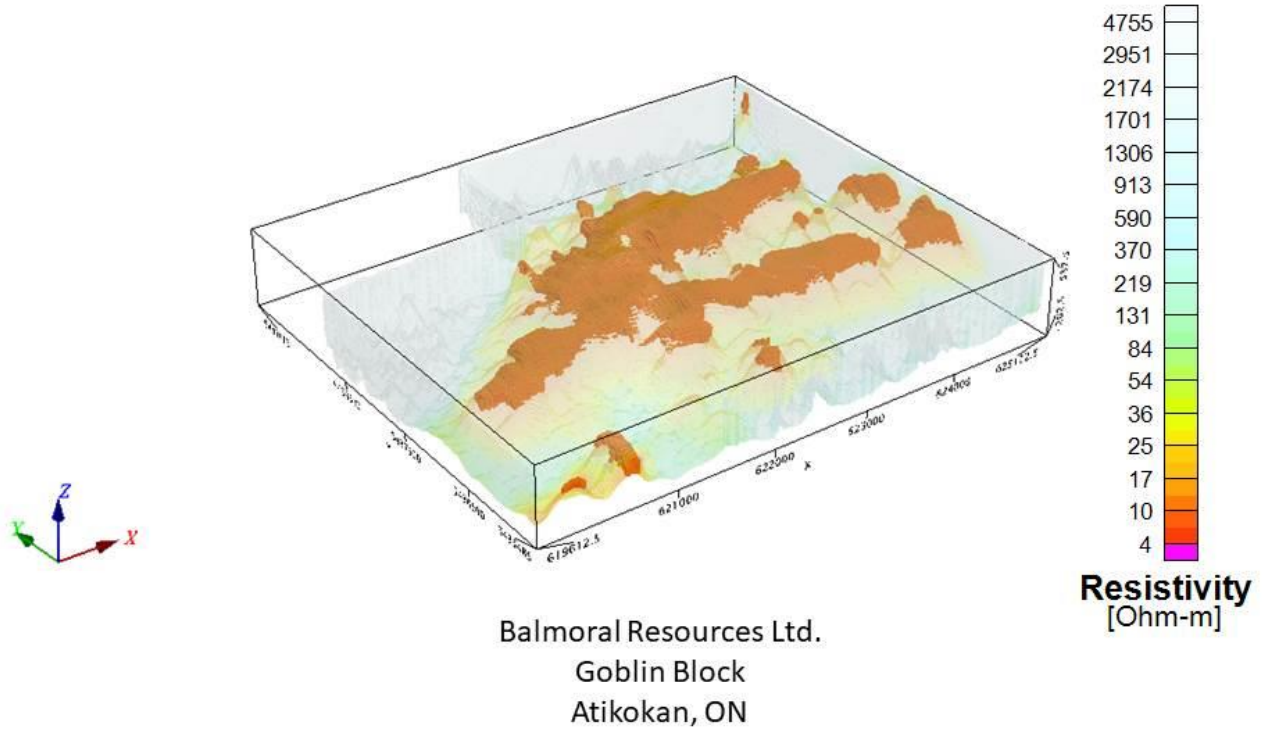
Total Magnetic Intensity (TMI) - Gargoyle



dB/dt Calculated Time Constant (Tau) - Gargoyle

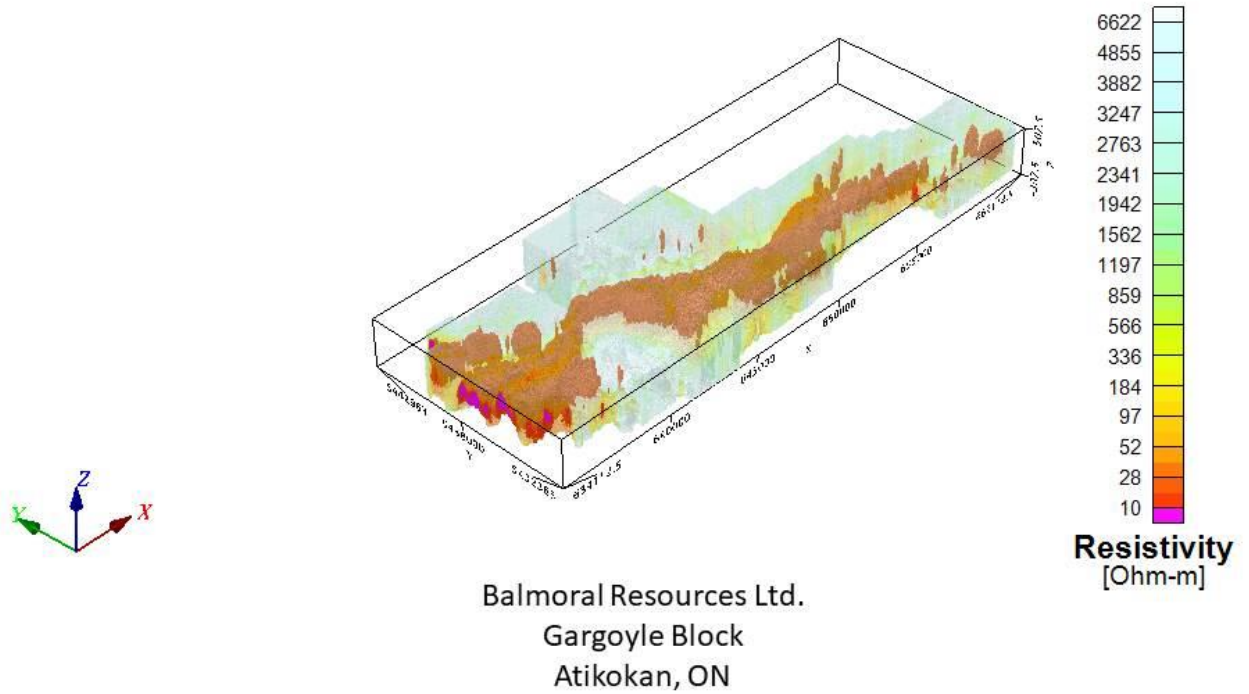
RESISTIVITY DEPTH IMAGE (RDI) MAPS

3D Apparent Resistivity



3D View of Apparent Resistivity Depth Imaging (RDI) - Goblin

3D Apparent Resistivity



3D View of Apparent Resistivity Depth Imaging (RDI) - Gargoyle

APPENDIX D

GENERALIZED MODELING RESULTS OF THE VTEM SYSTEM INTRODUCTION

The VTEM system is based on a concentric or central loop design, whereby, the receiver is positioned at the centre of a transmitter loop that produces a primary field. The wave form is a bi-polar, modified square wave with a turn-on and turn-off at each end.

During turn-on and turn-off, a time varying field is produced (dB/dt) and an electro-motive force (emf) is created as a finite impulse response. A current ring around the transmitter loop moves outward and downward as time progresses. When conductive rocks and mineralization are encountered, a secondary field is created by mutual induction and measured by the receiver at the centre of the transmitter loop.

Efficient modeling of the results can be carried out on regularly shaped geometries, thus yielding close approximations to the parameters of the measured targets. The following is a description of a series of common models made for the purpose of promoting a general understanding of the measured results.

A set of models has been produced for the Geotech VTEM™ system dB/dT Z and X components (see models D1 to D15). The Maxwell™ modeling program (EMIT Technology Pty. Ltd. Midland, WA, AU) used to generate the following responses assumes a resistive half-space. The reader is encouraged to review these models, so as to get a general understanding of the responses as they apply to survey results. While these models do not begin to cover all possibilities, they give a general perspective on the simple and most commonly encountered anomalies.

As the plate dips and departs from the vertical position, the peaks become asymmetrical.

As the dip increases, the aspect ratio (Min/Max) decreases and this aspect ratio can be used as an empirical guide to dip angles from near 90° to about 30°. The method is not sensitive enough where dips are less than about 30°.

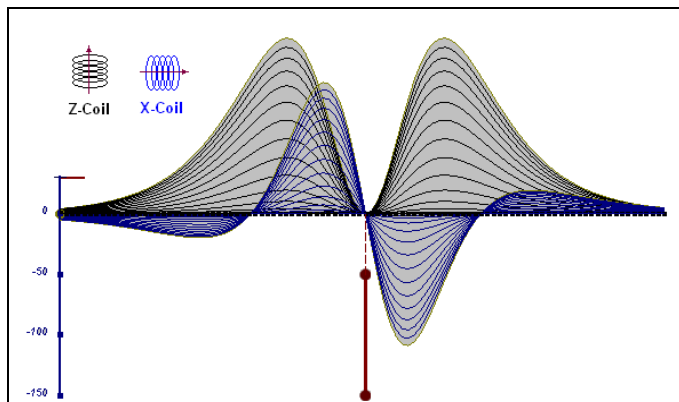


Figure D-1: vertical thin plate

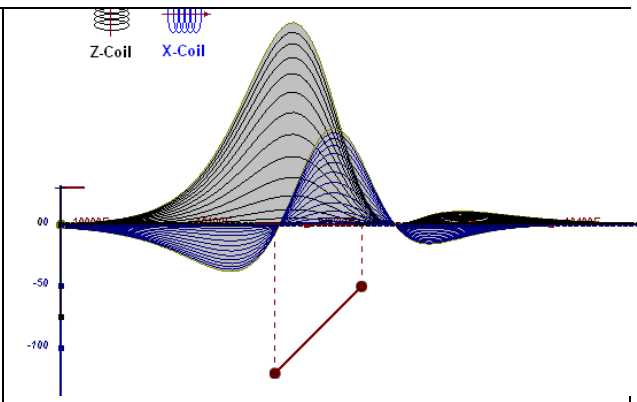


Figure D-2: inclined thin plate

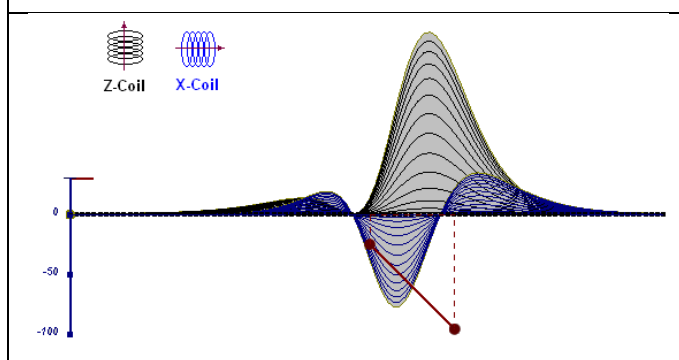


Figure D-3: inclined thin plate

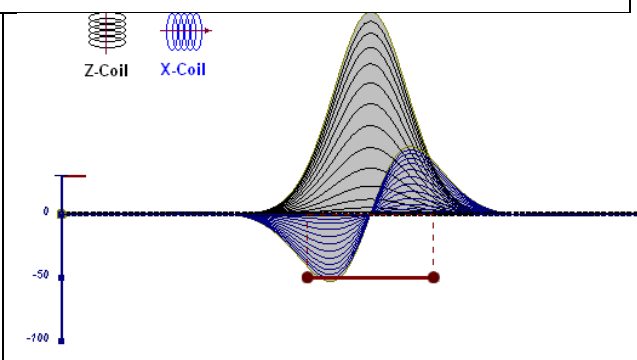


Figure D-4: horizontal thin plate

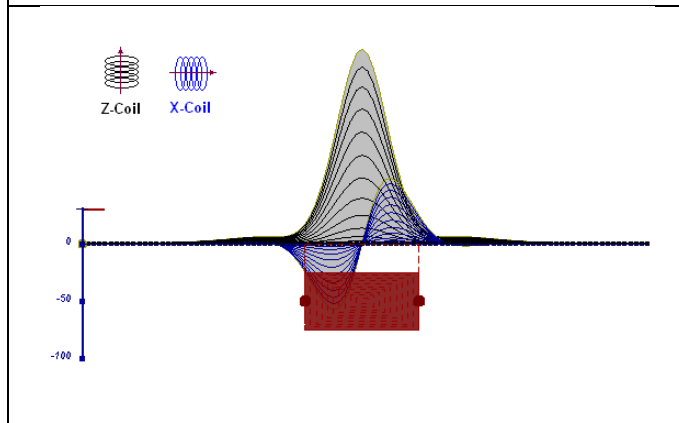


Figure D-5: horizontal thick plate (linear scale of the response)

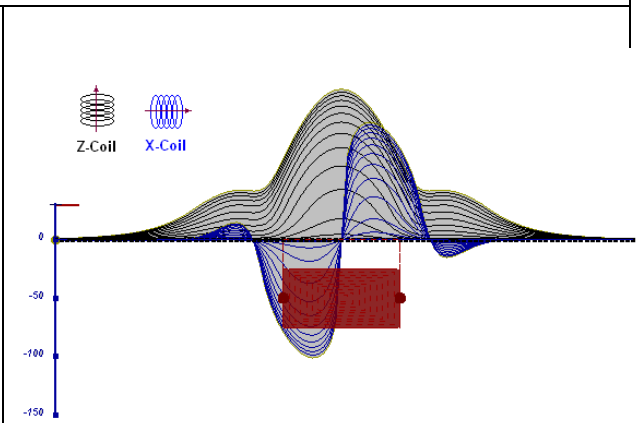


Figure D-6: horizontal thick plate (log scale of the response)

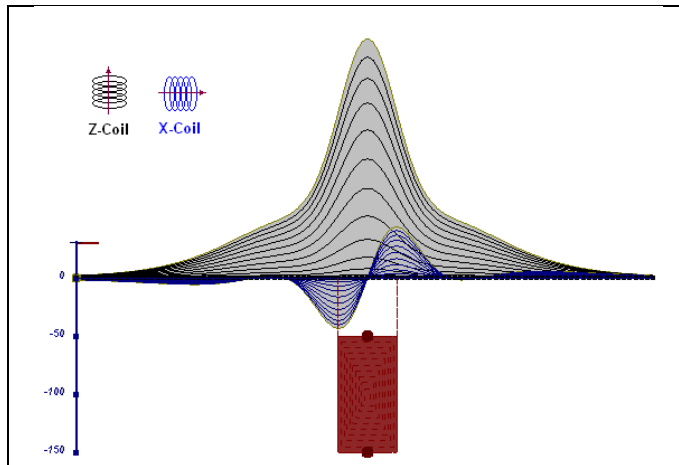


Figure D-7: vertical thick plate (linear scale of the response). 50 m depth

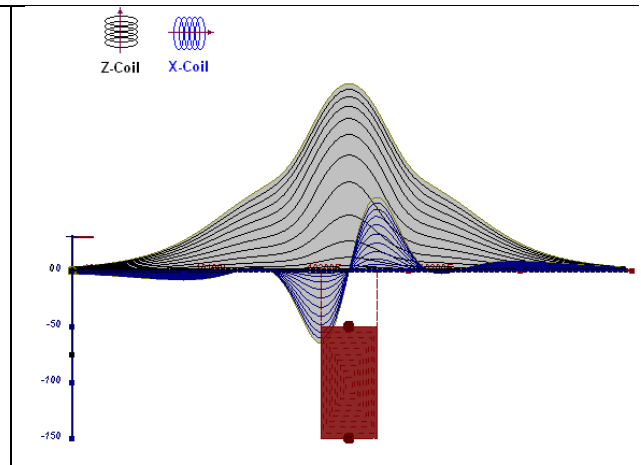


Figure D-8: vertical thick plate (log scale of the response). 50 m depth

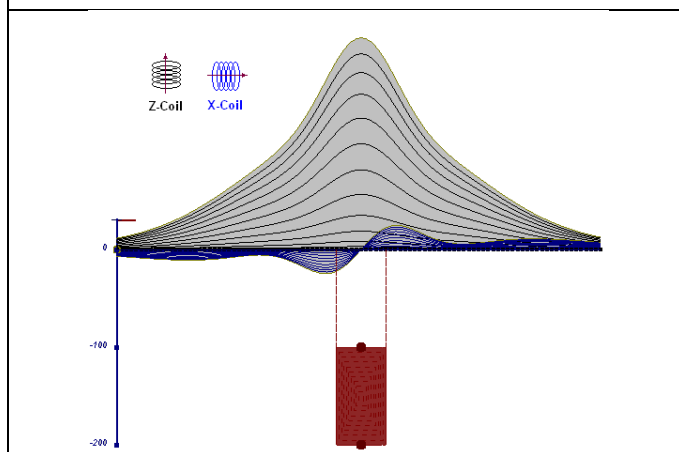


Figure D-9: vertical thick plate (linear scale of the response). 100 m depth

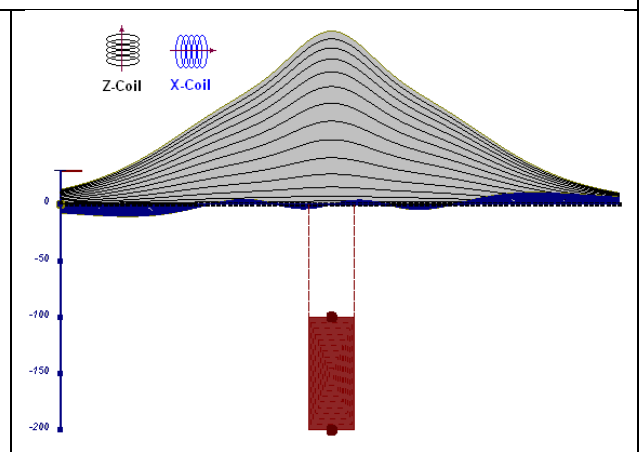


Figure D-10: vertical thick plate (linear scale of the response). Depth / horizontal thickness=2.5

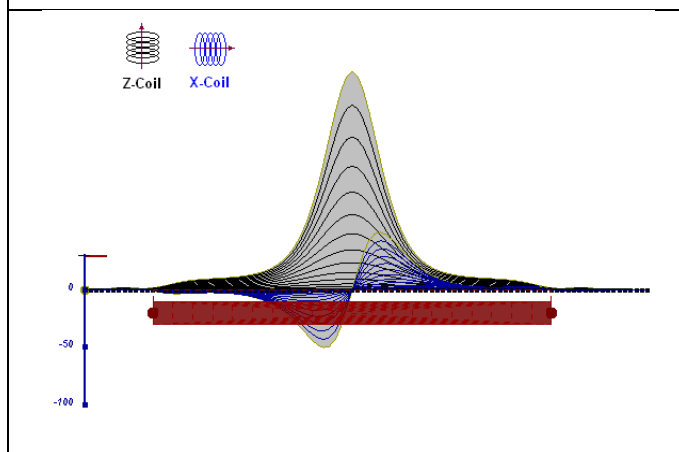


Figure D-11: horizontal thick plate (linear scale of the response)

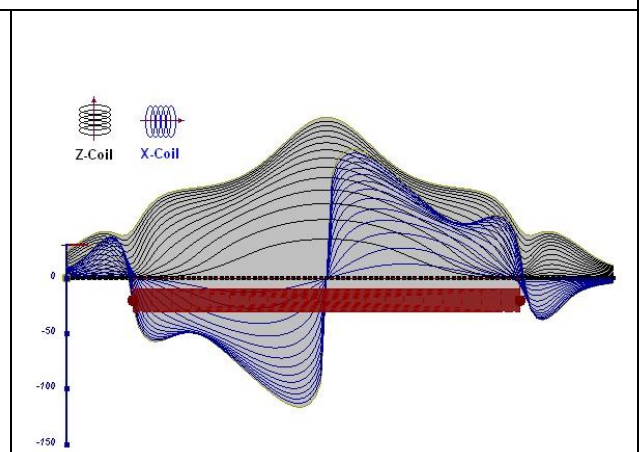


Figure D-12: horizontal thick plate (log scale of the response)

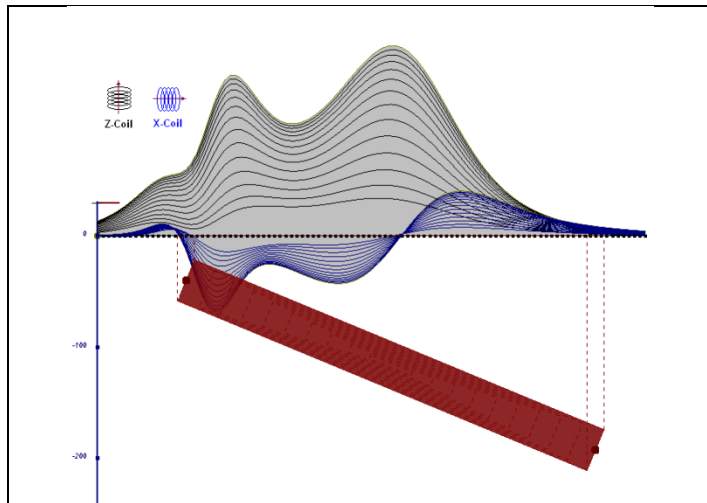


Figure D-13: inclined long thick plate

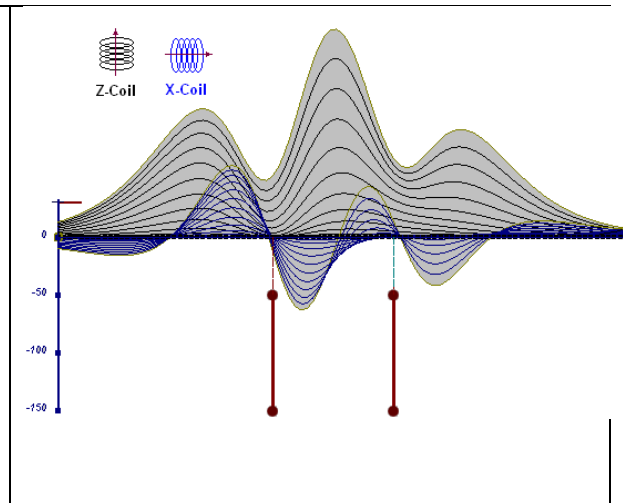


Figure D-14: two vertical thin plates

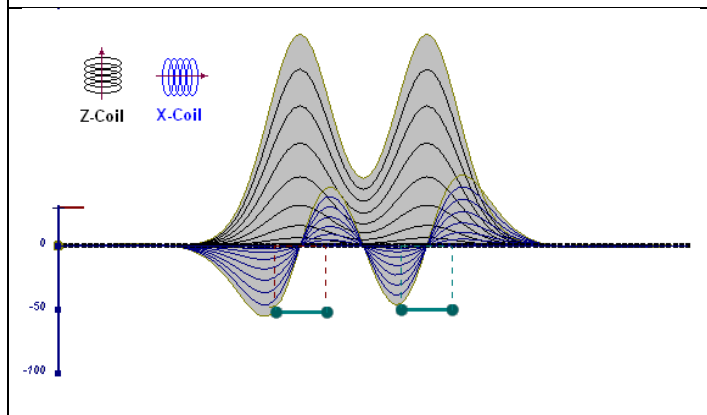


Figure D-15: two horizontal thin plates

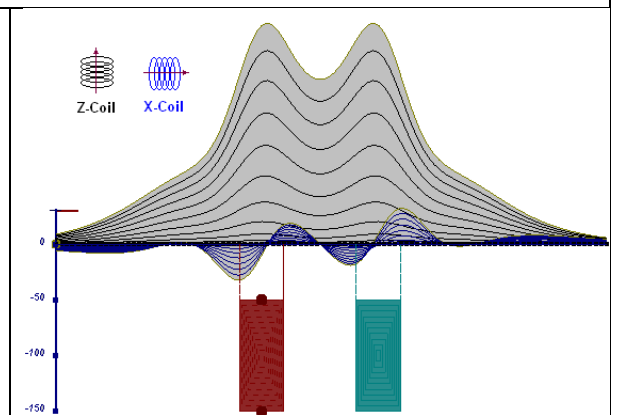


Figure D-16: two vertical thick plates

The same type of target but with different thickness, for example, creates different form of the response:

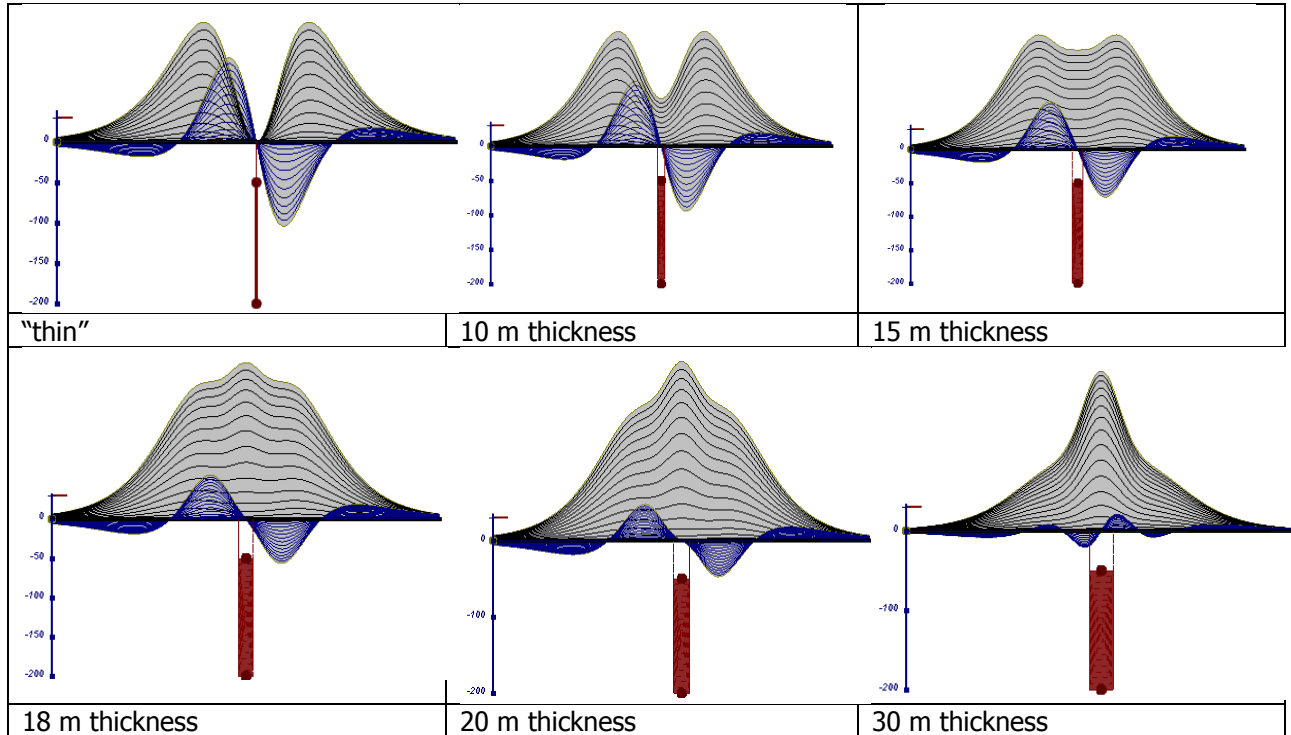


Figure D-17: Conductive vertical plate, depth 50 m, strike length 200 m, depth extends 150 m.

Alexander Prikhodko, PhD, P.Ge
Geotech Ltd.

September 2010

APPENDIX E

EM TIME CONSTANT (TAU) ANALYSIS

Estimation of time constant parameter¹ in transient electromagnetic method is one of the steps toward the extraction of the information about conductances beneath the surface from TEM measurements.

The most reliable method to discriminate or rank conductors from overburden, background or one and other is by calculating the EM field decay time constant (TAU parameter), which directly depends on conductance despite their depth and accordingly amplitude of the response.

THEORY

As established in electromagnetic theory, the magnitude of the electro-motive force (emf) induced is proportional to the time rate of change of primary magnetic field at the conductor. This emf causes eddy currents to flow in the conductor with a characteristic transient decay, whose Time Constant (Tau) is a function of the conductance of the survey target or conductivity and geometry (including dimensions) of the target. The decaying currents generate a proportional secondary magnetic field, the time rate of change of which is measured by the receiver coil as induced voltage during the Off time.

The receiver coil output voltage (e_0) is proportional to the time rate of change of the secondary magnetic field and has the form,

$$e_0 \propto (1 / \tau) e^{-(t / \tau)}$$

Where,

$\tau = L/R$ is the characteristic time constant of the target (TAU)

R = resistance

L = inductance

From the expression, conductive targets that have small value of resistance and hence large value of τ yield signals with small initial amplitude that decays relatively slowly with progress of time. Conversely, signals from poorly conducting targets that have large resistance value and small τ , have high initial amplitude but decay rapidly with time¹ (Fig. E1).

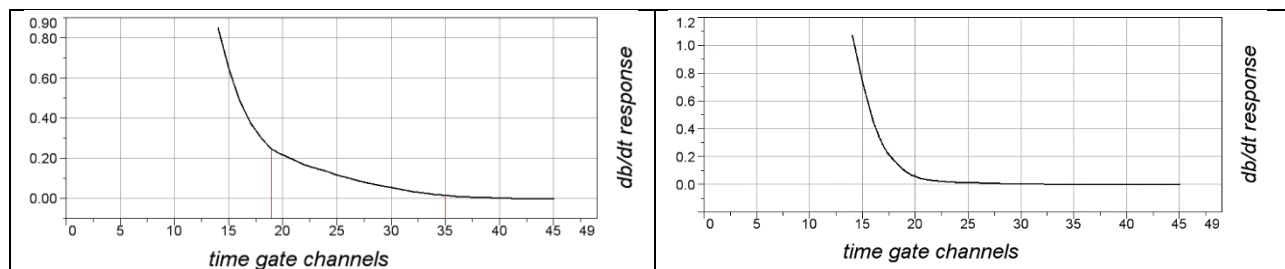


Figure E-1: Left – presence of good conductor, right – poor conductor.

¹ McNeill, JD, 1980, "Applications of Transient Electromagnetic Techniques", Technical Note TN-7 page 5, Geonics Limited, Mississauga, Ontario.

EM Time Constant (Tau) Calculation

The EM Time-Constant (TAU) is a general measure of the speed of decay of the electromagnetic response and indicates the presence of eddy currents in conductive sources as well as reflecting the “conductance quality” of a source. Although TAU can be calculated using either the measured dB/dt decay or the calculated B-field decay, dB/dt is commonly preferred due to better stability (S/N) relating to signal noise. Generally, TAU calculated on base of early time response reflects both near surface overburden and poor conductors whereas, in the late ranges of time, deep and more conductive sources, respectively. For example early time TAU distribution in an area that indicates conductive overburden is shown in Figure 2.

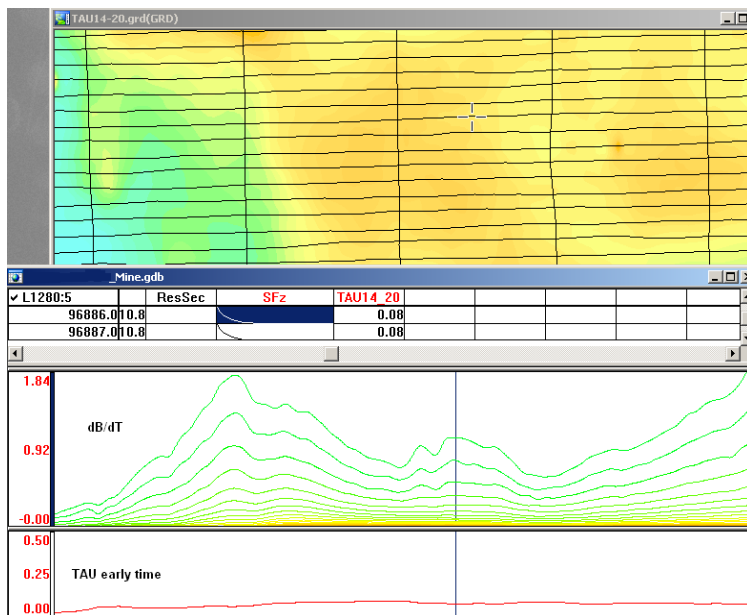


Figure E-2: Map of early time TAU. Area with overburden conductive layer and local sources.

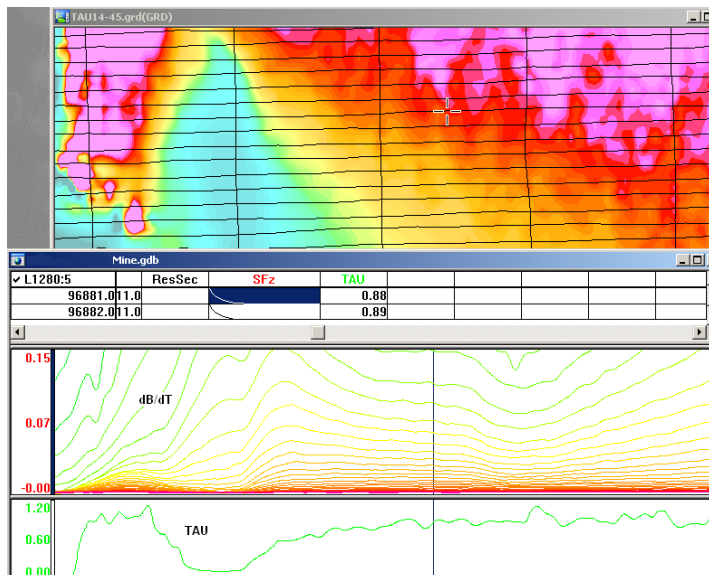


Figure E-3: Map of full time range TAU with EM anomaly due to deep highly conductive target.

There are many advantages of TAU maps:

- TAU depends only on one parameter (conductance) in contrast to response magnitude;
- TAU is integral parameter, which covers time range and all conductive zones and targets are displayed independently of their depth and conductivity on a single map.
- Very good differential resolution in complex conductive places with many sources with different conductivity.
- Signs of the presence of good conductive targets are amplified and emphasized independently of their depth and level of response accordingly.

In the example shown in Figure 4 and 5, three local targets are defined, each of them with a different depth of burial, as indicated on the resistivity depth image (RDI). All are very good conductors but the deeper target (number 2) has a relatively weak dB/dt signal yet also features the strongest total TAU (Figure 4). This example highlights the benefit of TAU analysis in terms of an additional target discrimination tool.

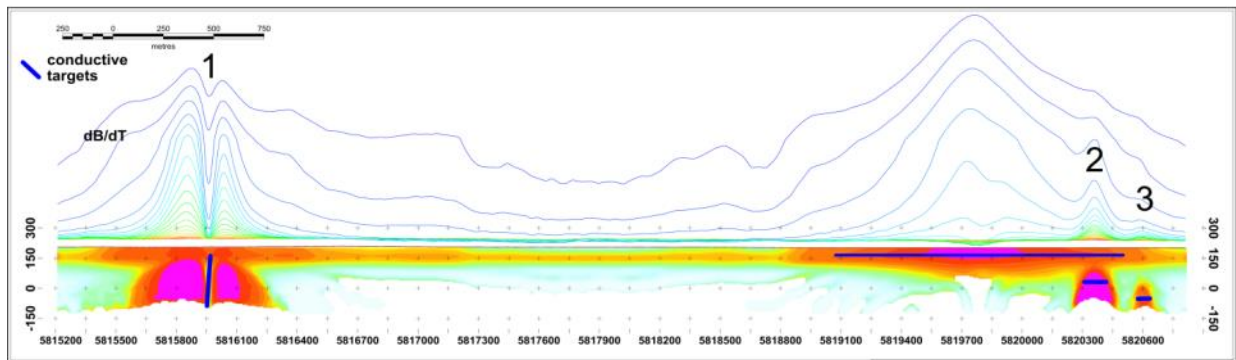


Figure E-4: dB/dt profile and RDI with different depths of targets.

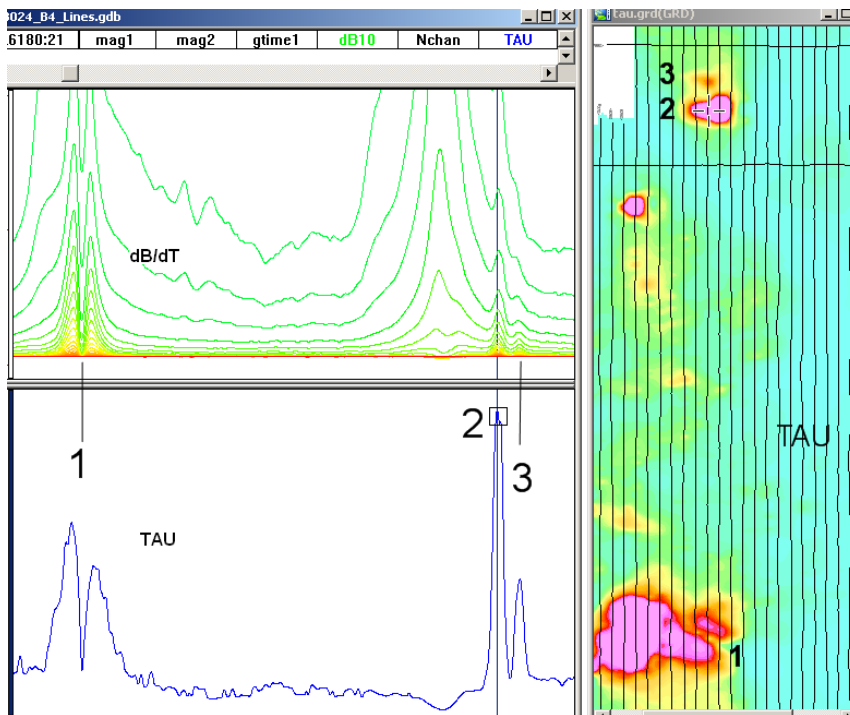


Figure E-5: Map of total TAU and dB/dt profile.

The EM Time Constants for dB/dt and B-field were calculated using the “sliding Tau” in-house program developed at Geotech2. The principle of the calculation is based on using of time window (4 time channels) which is sliding along the curve decay and looking for latest time channels which have a response above the level of noise and decay. The EM decays are obtained from all available decay channels, starting at the latest channel. Time constants are taken from a least square fit of a straight-line (log/linear space) over the last 4 gates above a pre-set signal threshold level (Figure F6). Threshold settings are pointed in the “label” property of TAU database channels. The sliding Tau method determines that, as the amplitudes increase, the time-constant is taken at progressively later times in the EM decay. Conversely, as the amplitudes decrease, Tau is taken at progressively earlier times in the decay. If the maximum signal amplitude falls below the threshold, or becomes negative for any of the 4 time gates, then Tau is not calculated and is assigned a value of “dummy” by default.

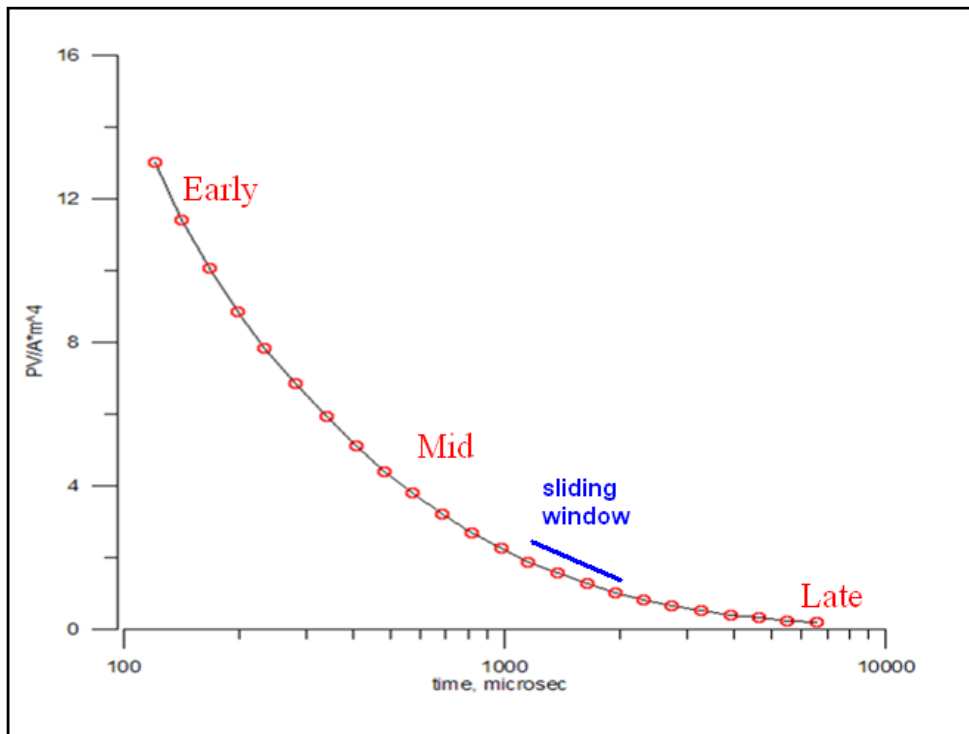


Figure E-6: Typical dB/dt decays of Vtem data

Alexander Prikhodko, PhD, P.Geo
Geotech Ltd.

September 2010

² by A.Prikhodko

APPENDIX F

TEM RESISTIVITY DEPTH IMAGING (RDI)

Resistivity depth imaging (RDI) is a technique used to rapidly convert EM profile decay data into an equivalent resistivity versus depth cross-section, by deconvolving the measured TEM data. The used RDI algorithm of Resistivity-Depth transformation is based on the scheme of the apparent resistivity transform of Maxwell A.Meju (1998)¹ and TEM response from a conductive half-space. The program is developed by Alexander Prikhodko and is depth calibrated based on forward plate modeling for VTEM system configuration (Fig. 1-10).

RDIs provide reasonable indications of conductor relative depth and vertical extent, as well as accurate 1D layered-earth apparent conductivity/resistivity structure across VTEM flight lines. Approximate depth of investigation of a TEM system, image of secondary field distribution in half-space, effective resistivity, initial geometry and position of conductive targets is the information obtained on the basis of the RDIs.

Maxwell forward modeling with RDI sections from the synthetic responses (VTEM system).

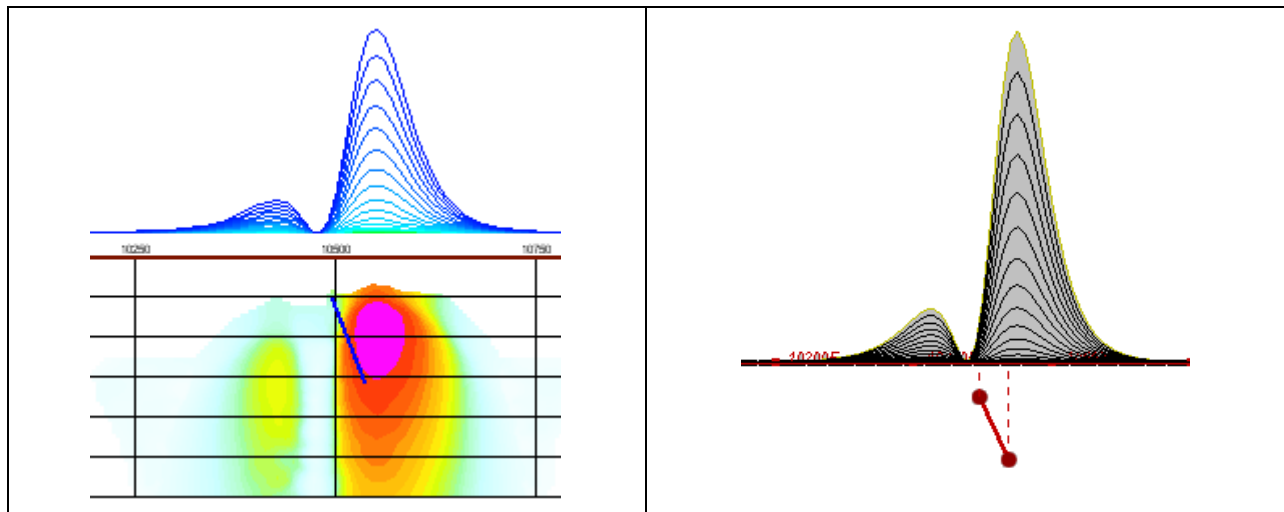


Figure F-1: Maxwell plate model and RDI from the calculated response for a conductive “thin” plate (depth 50 m, dip 65 degree, depth extend 100 m).

¹ Maxwell A.Meju, 1998, Short Note: A simple method of transient electromagnetic data analysis, *Geophysics*, **63**, 405–410.

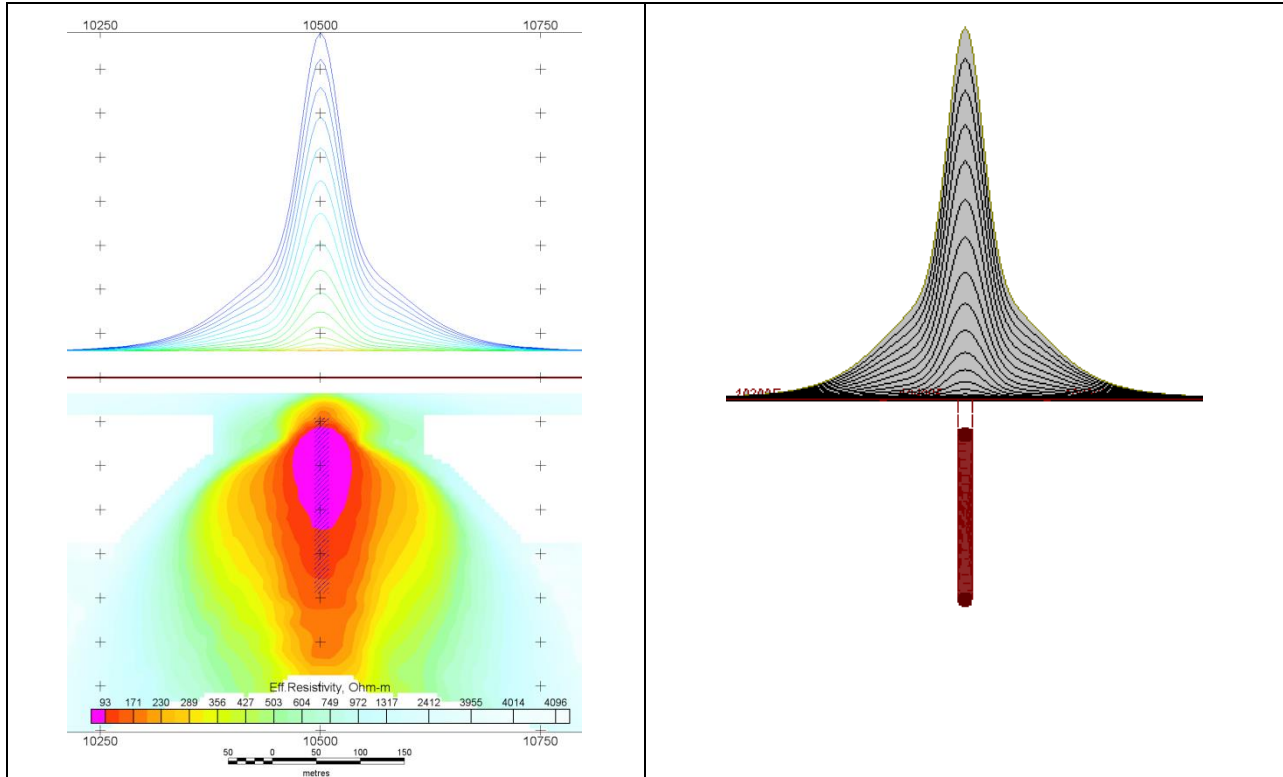


Figure F-2: Maxwell plate model and RDI from the calculated response for "thick" plate 18 m thickness, depth 50 m, depth extend 200 m).

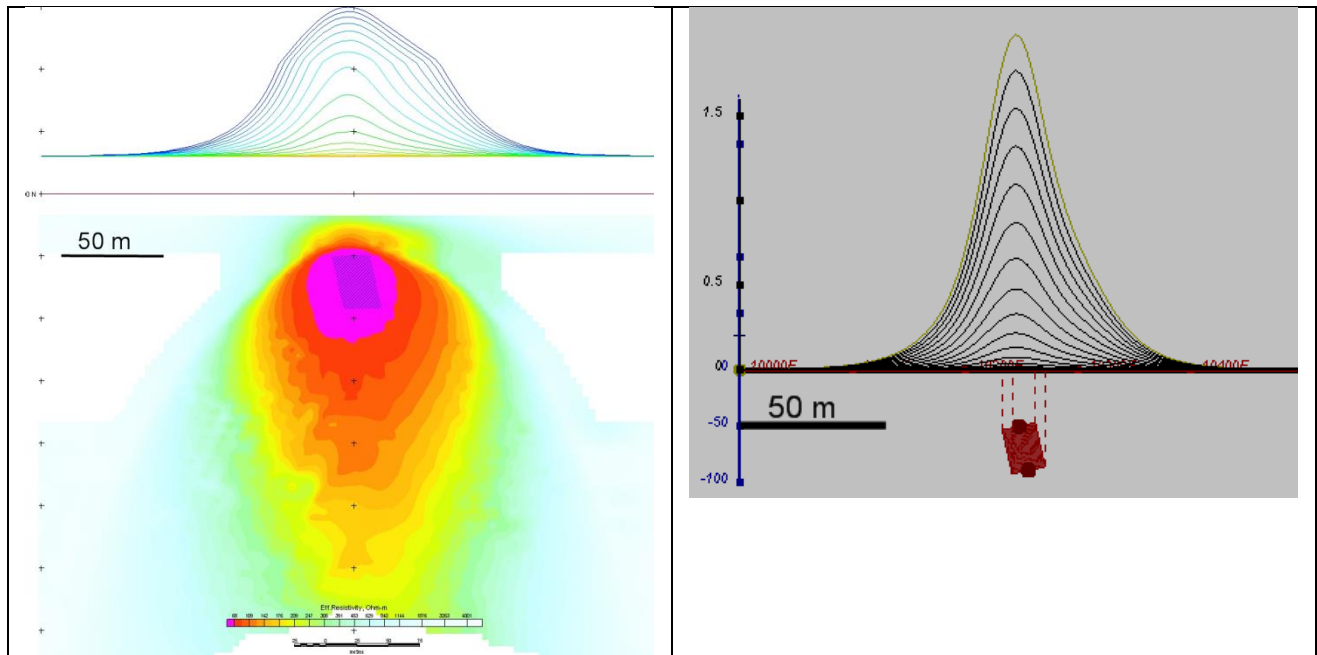


Figure F-3: Maxwell plate model and RDI from the calculated response for bulk ("thick") 100 m length, 40 m depth extend, 30 m thickness

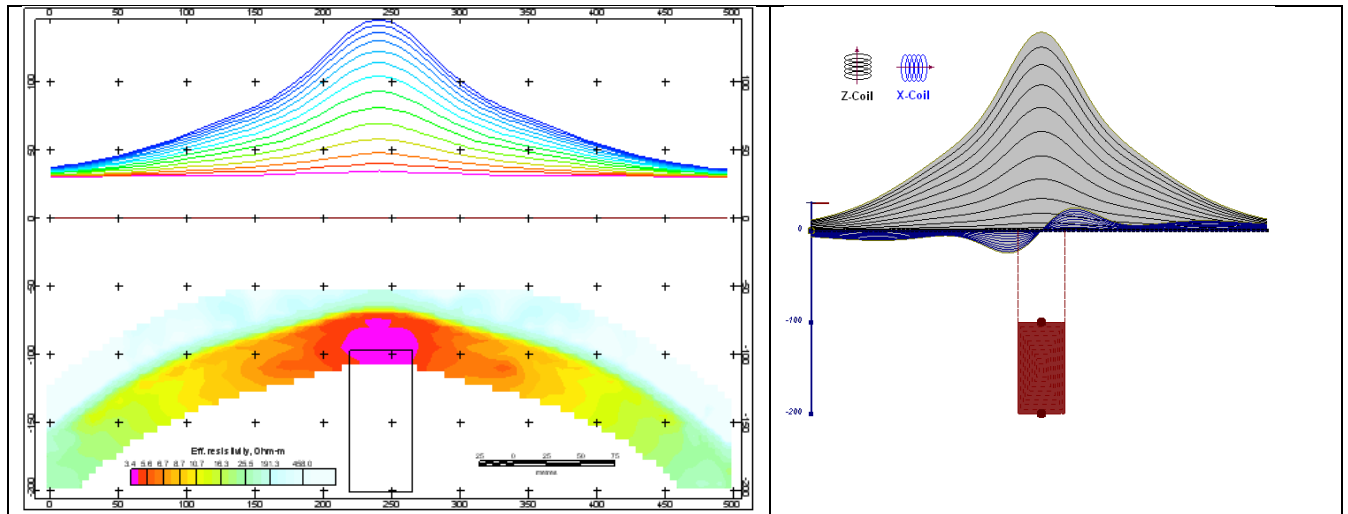


Figure F-4: Maxwell plate model and RDI from the calculated response for "thick" vertical target (depth 100 m, depth extend 100 m). 19-44 chan.

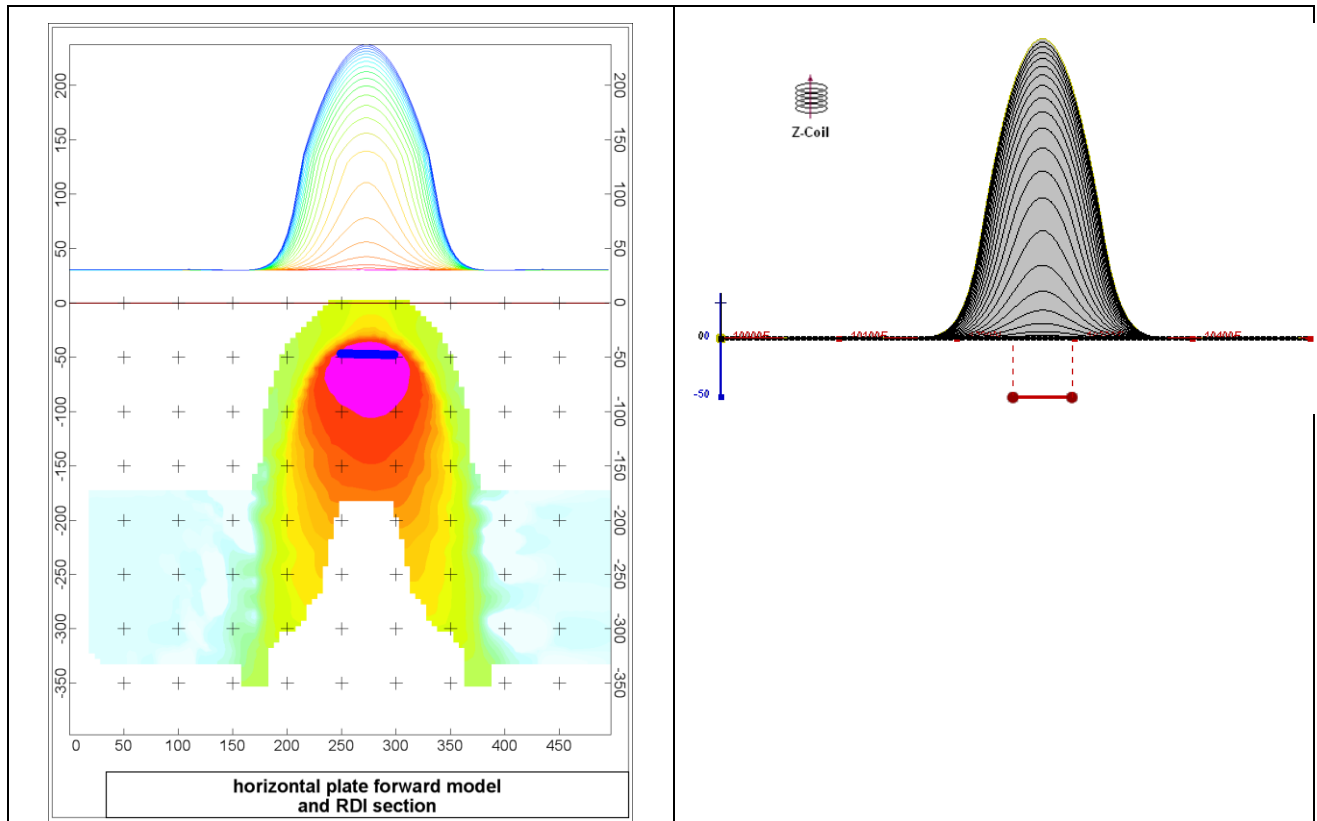


Figure F-5: Maxwell plate model and RDI from the calculated response for horizontal thin plate (depth 50 m, dim 50x100 m). 15-44 chan.

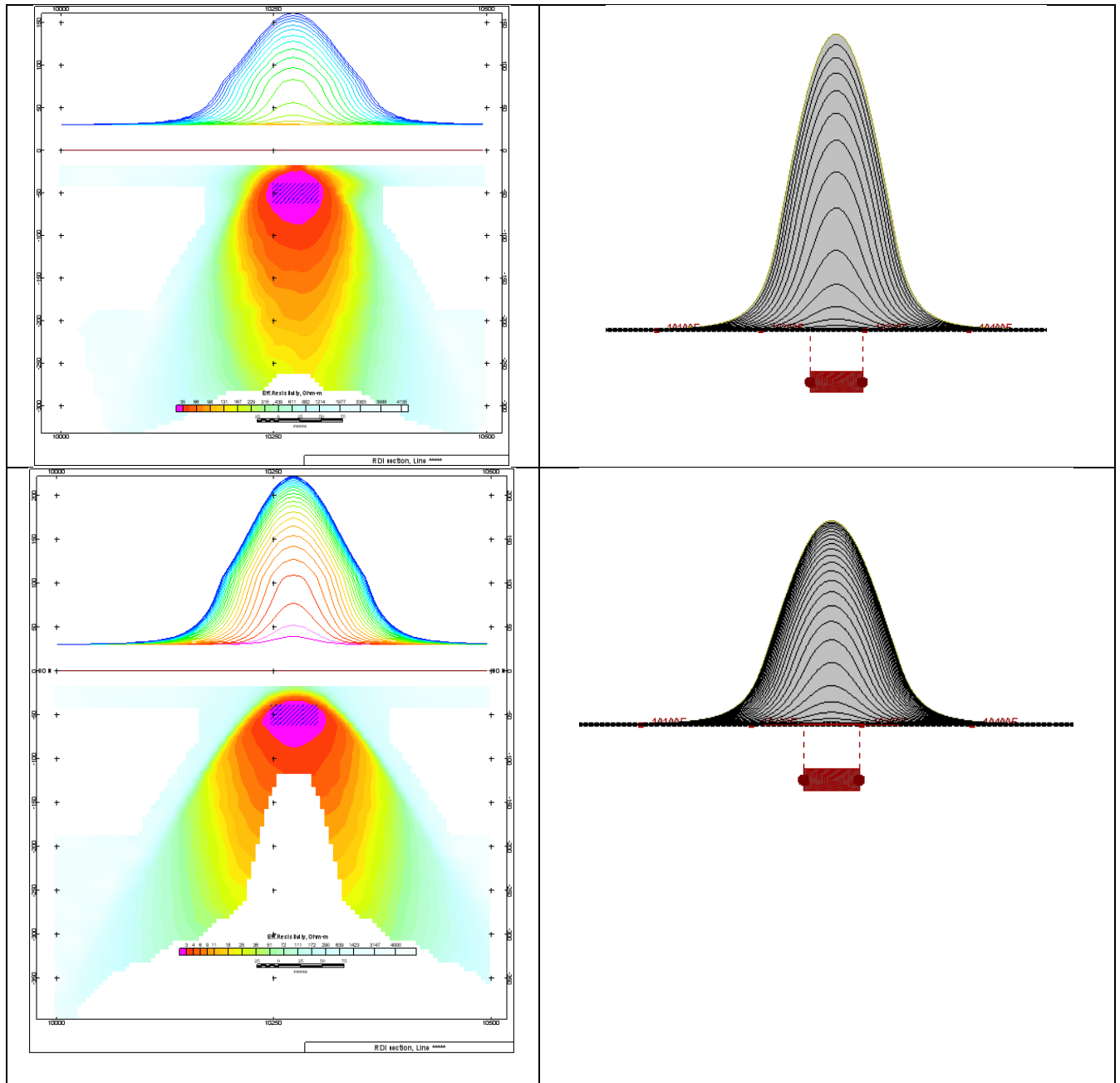


Figure F-6: Maxwell plate model and RDI from the calculated response for horizontal thick (20m) plate – less conductive (on the top), more conductive (below).

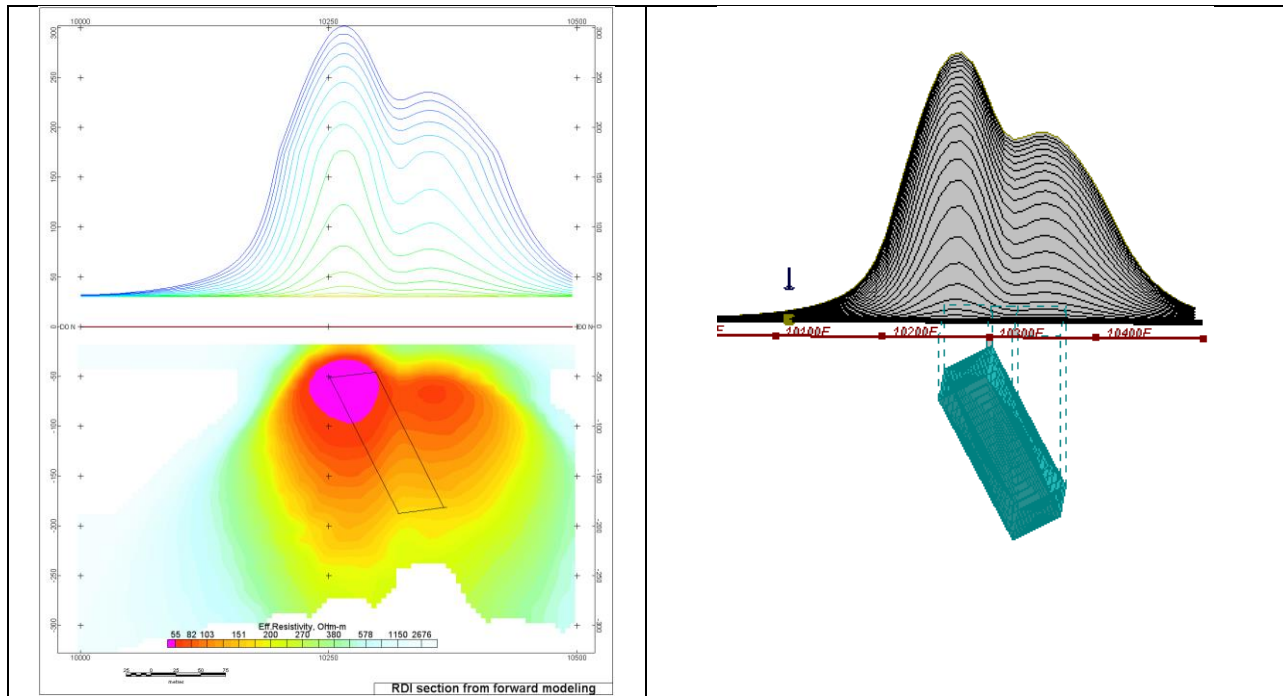


Figure F-7: Maxwell plate model and RDI from the calculated response for inclined thick (50m) plate. Depth extends 150 m, depth to the target 50 m.

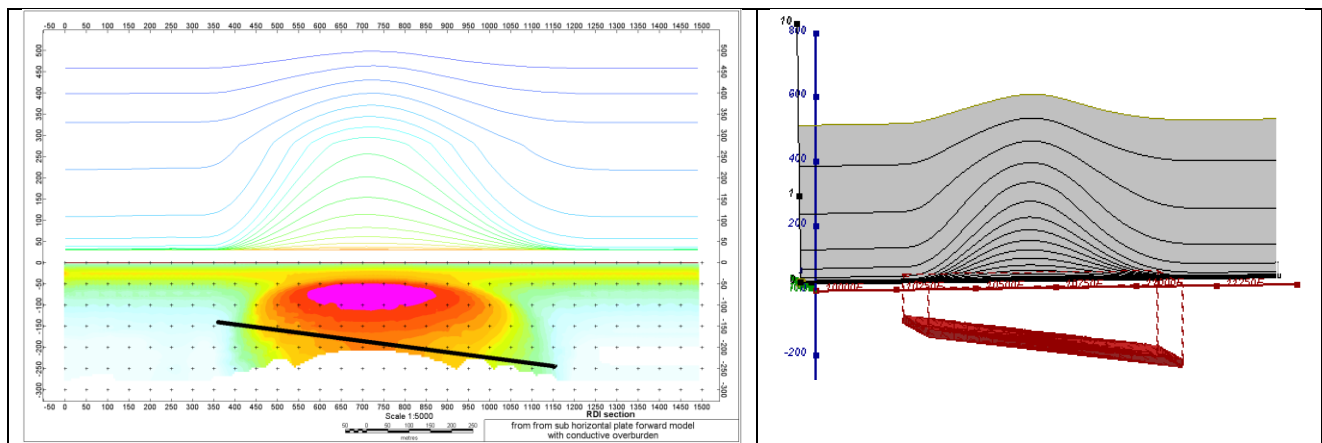


Figure F-8: Maxwell plate model and RDI from the calculated response for the long, wide and deep subhorizontal plate (depth 140 m, dim 25x500x800 m) with conductive overburden.

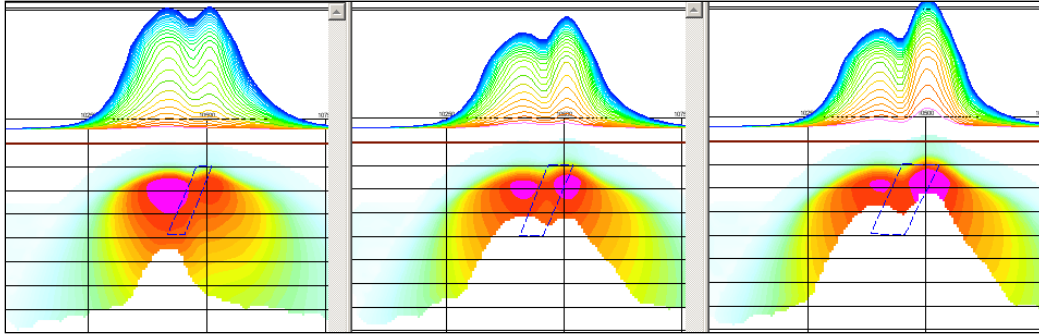


Figure F-9: Maxwell plate models and RDIs from the calculated response for "thick" dipping plates (35, 50, 75 m thickness), depth 50 m, conductivity 2.5 S/m.

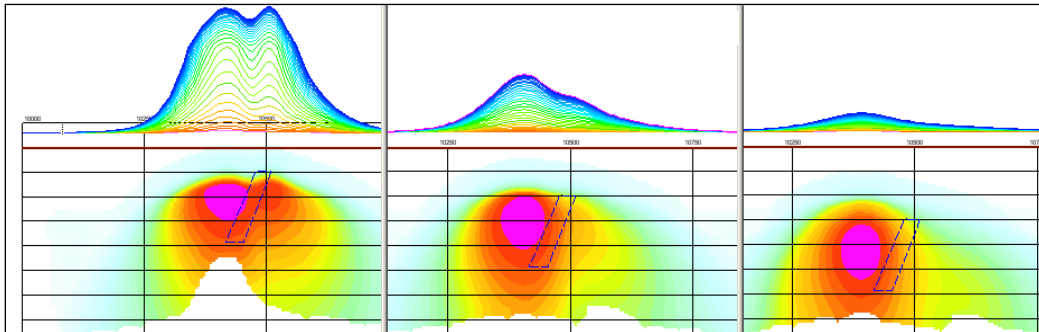


Figure F-10: Maxwell plate models and RDIs from the calculated response for "thick" (35 m thickness) dipping plate on different depth (50, 100, 150 m), conductivity 2.5 S/m.

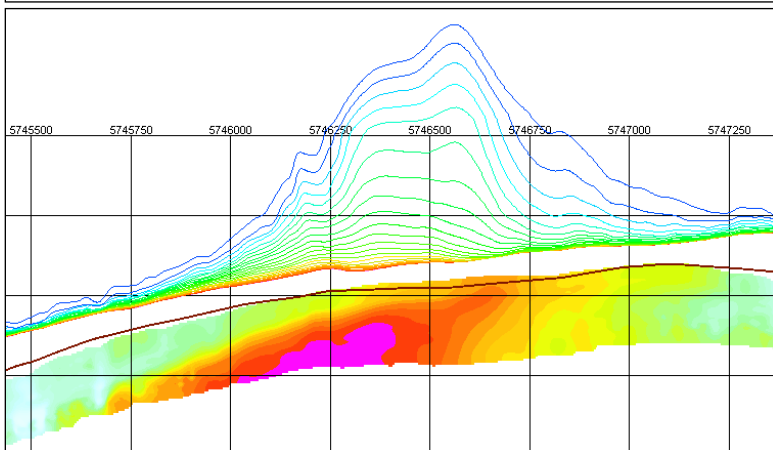
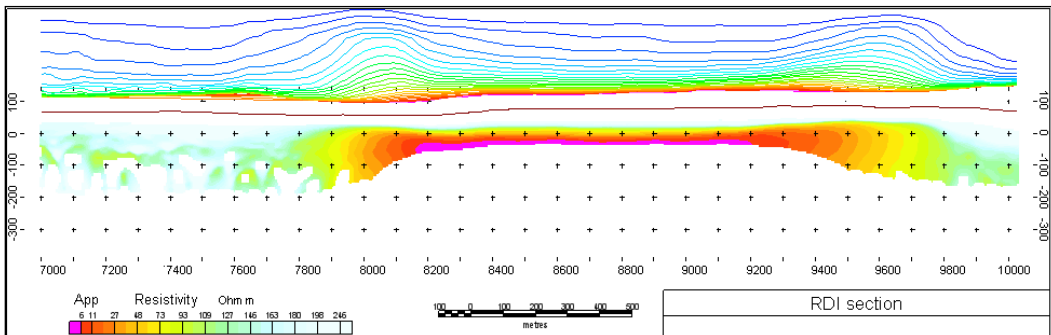
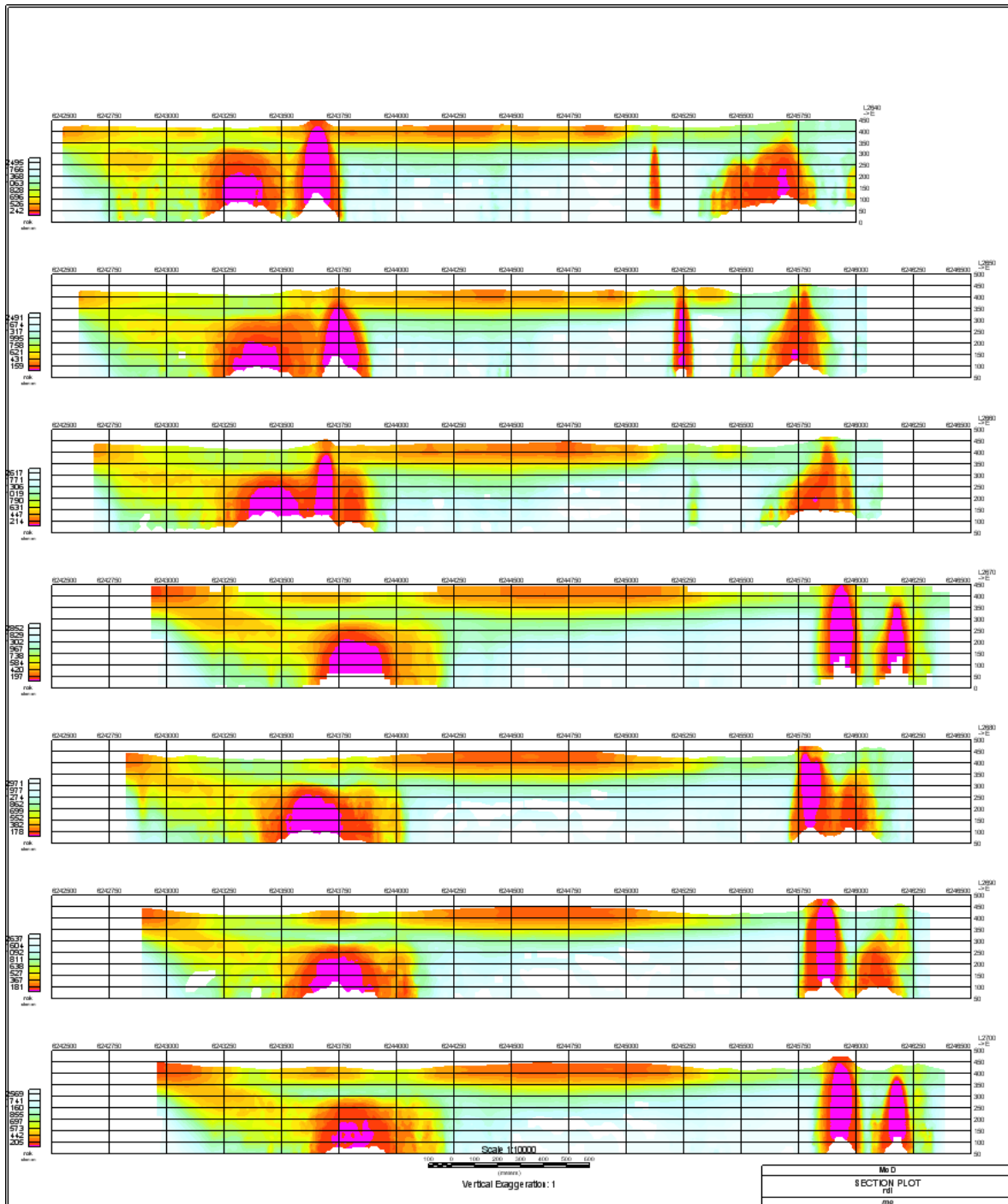


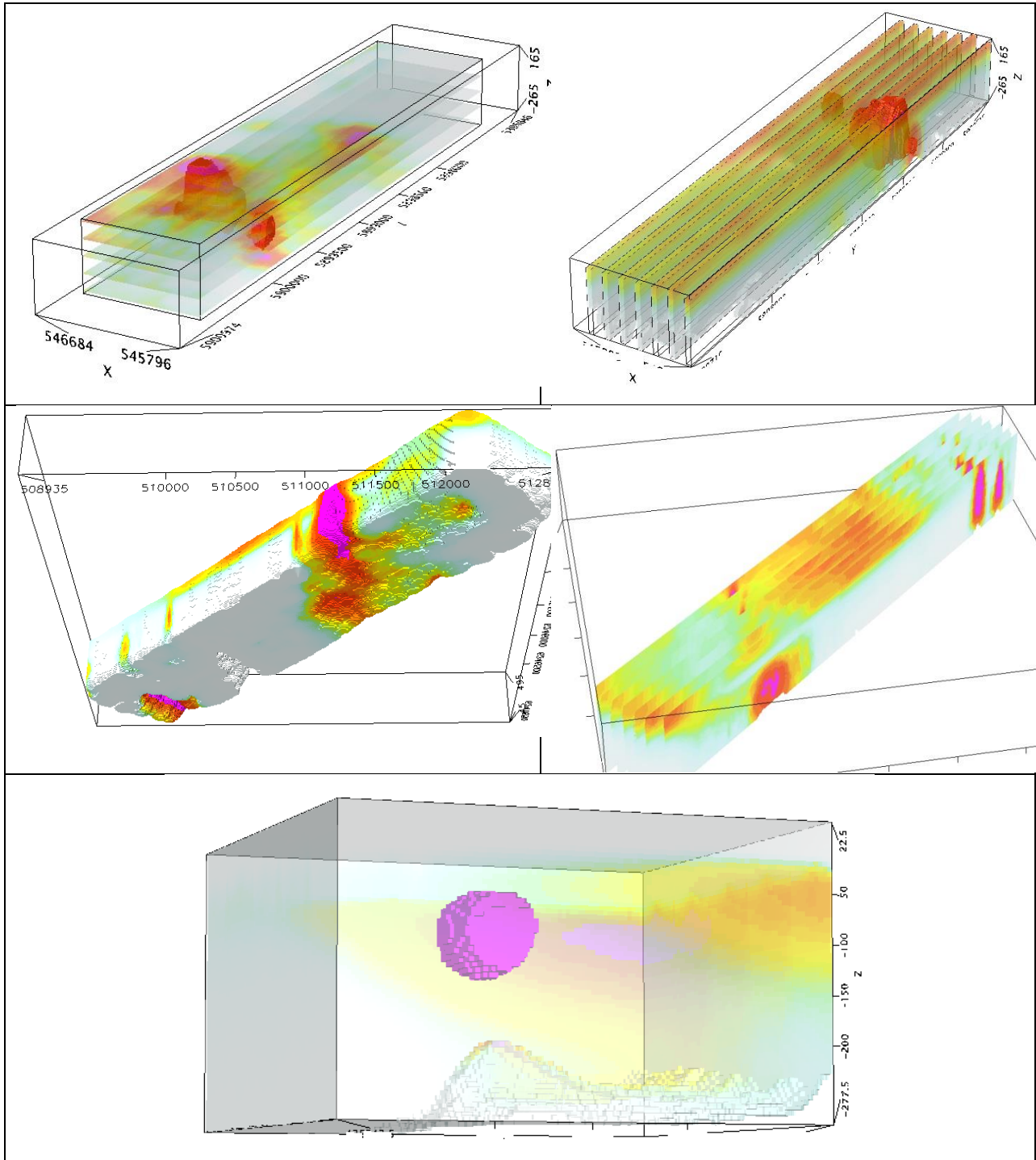
Figure F-11: RDI section for the real horizontal and slightly dipping conductive layers

FORMS OF RDI PRESENTATION

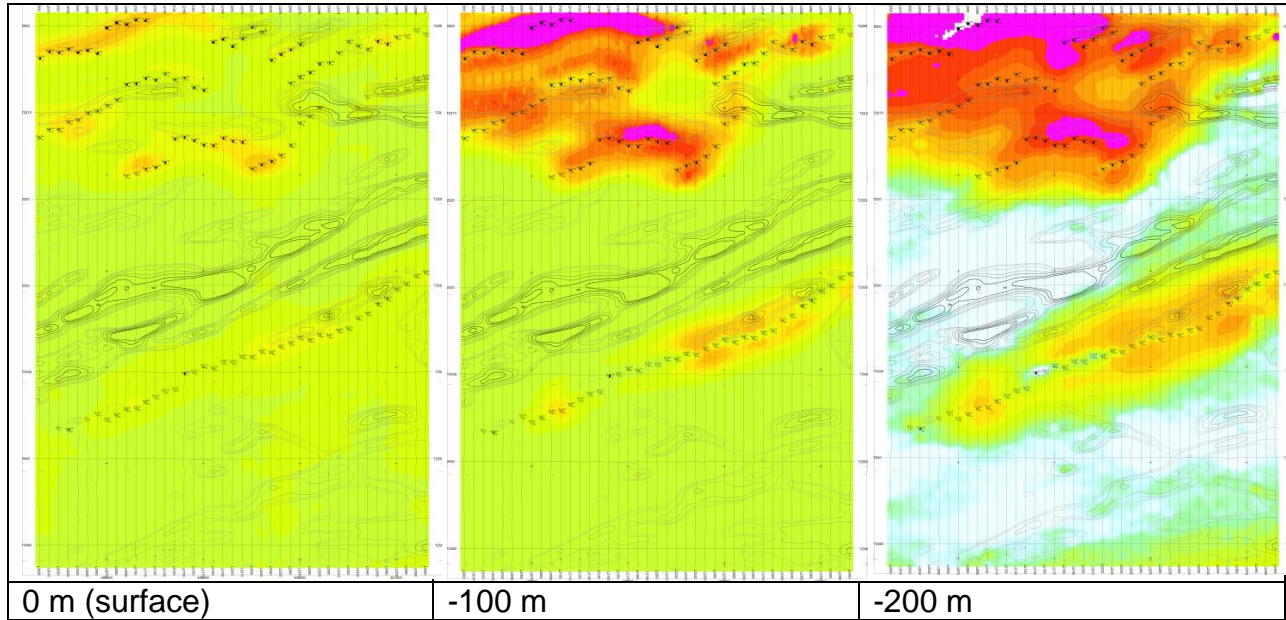
PRESENTATION OF SERIES OF LINES



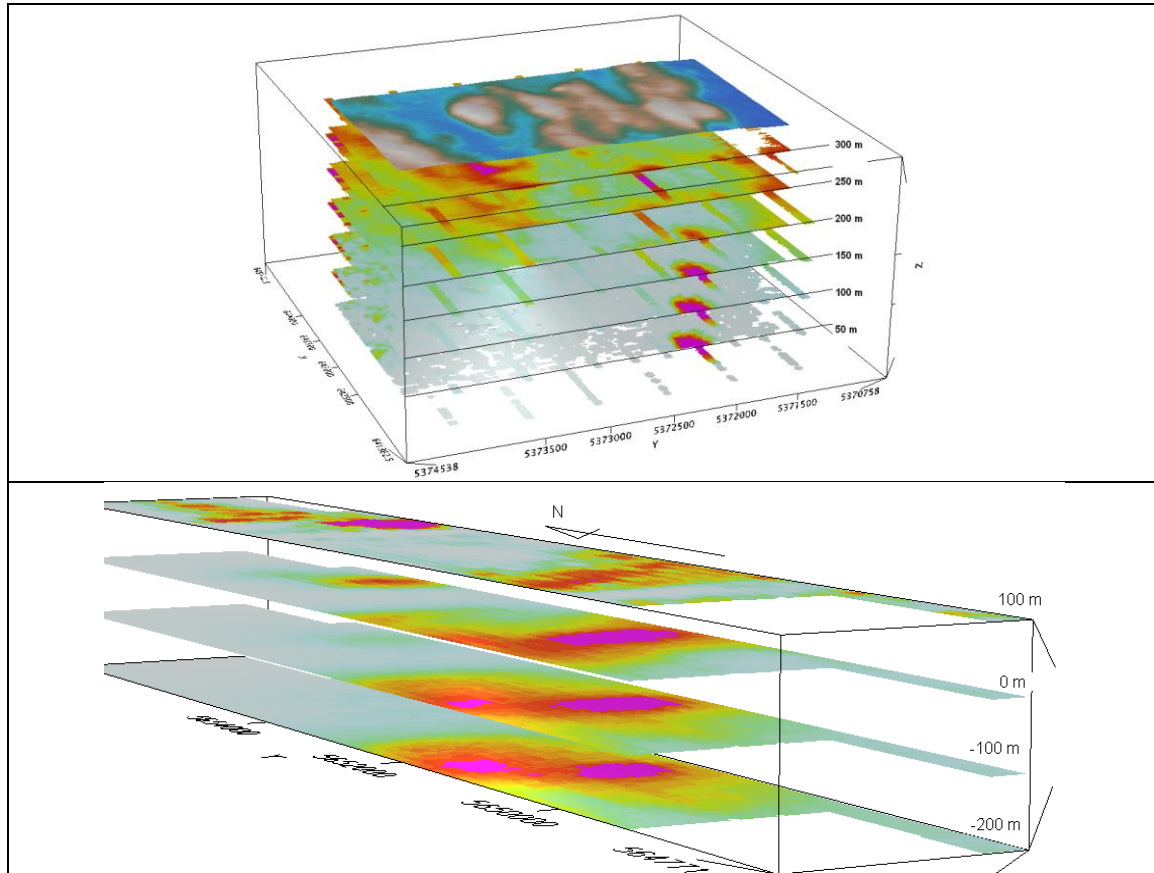
3D PRESENTATION OF RDIS



APPARENT RESISTIVITY DEPTH SLICES PLANS:

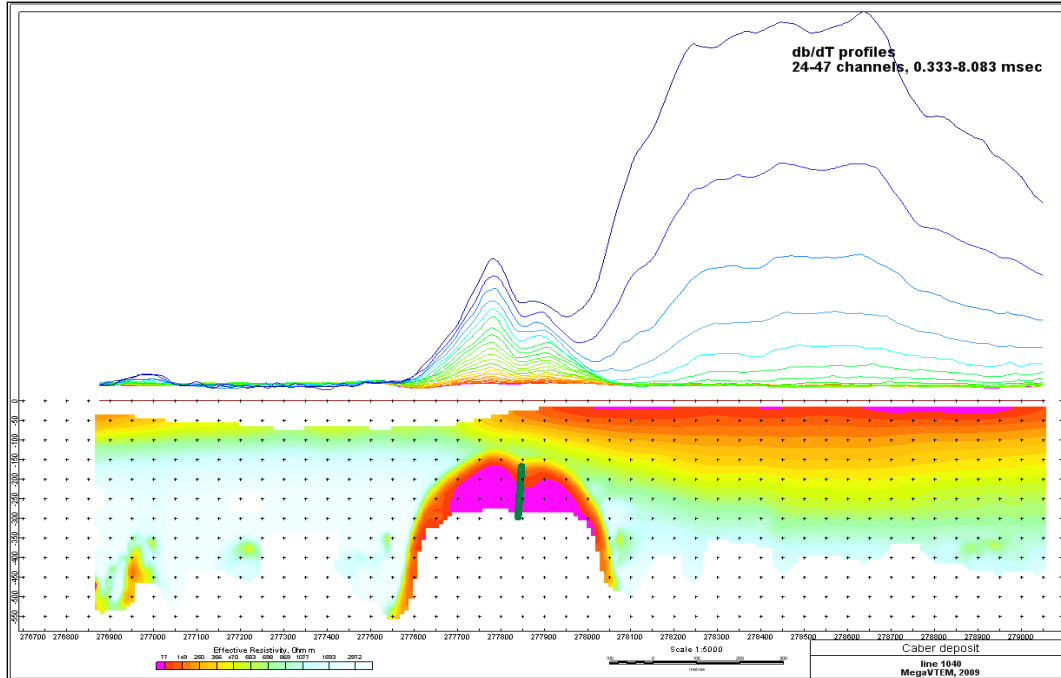


3D VIEWS OF APPARENT RESISTIVITY DEPTH SLICES:

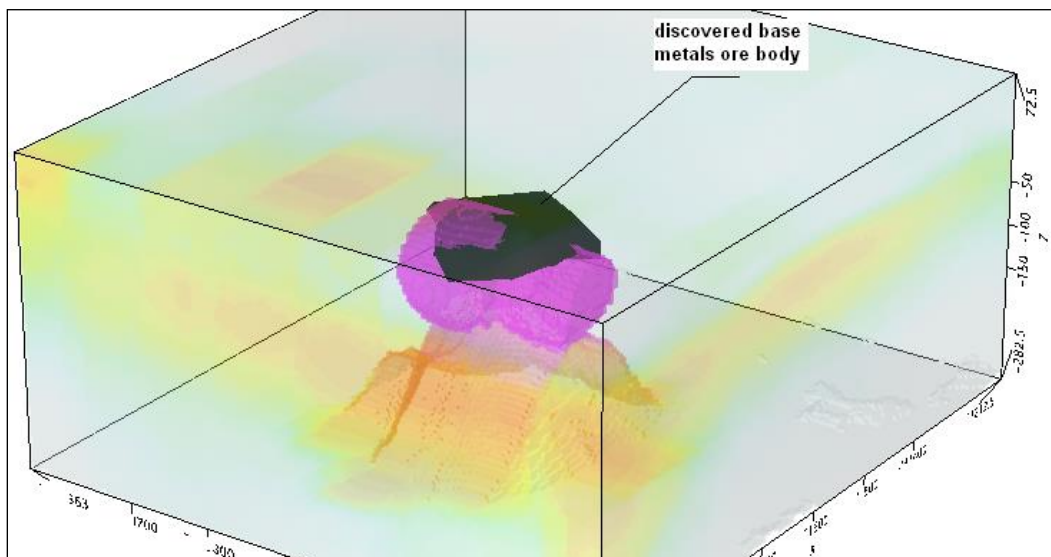


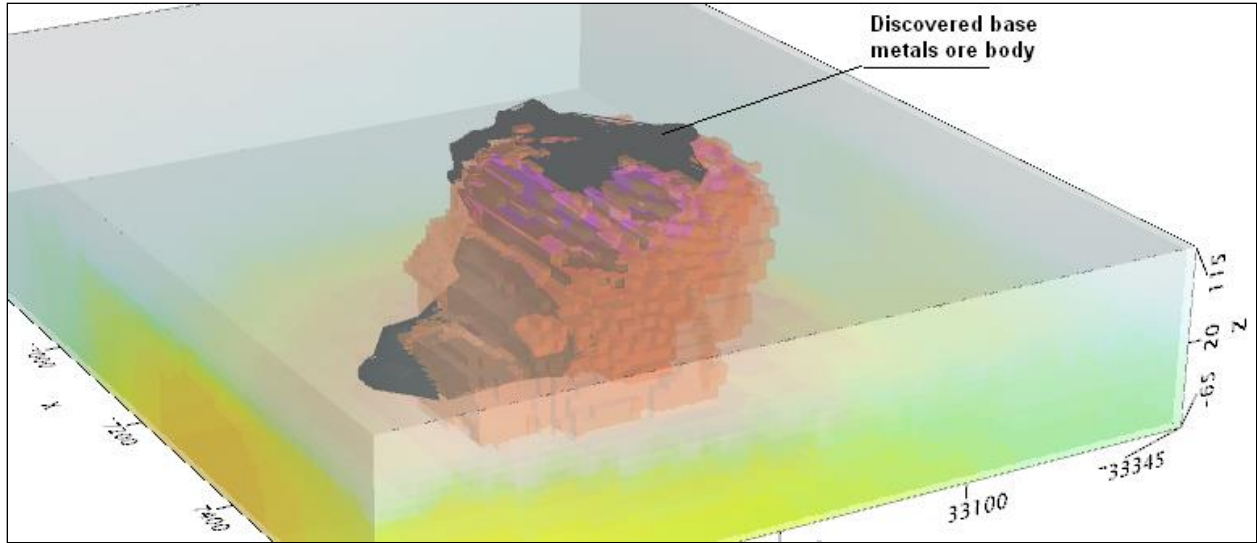
REAL BASE METAL TARGETS IN COMPARISON WITH RDIS:

RDI section of the line over Caber deposit ("thin" subvertical plate target and conductive overburden).



3D RDI VOXELS WITH BASE METALS ORE BODIES (MIDDLE EAST):





Alexander Prikhodko, PhD, P.Ge
Geotech Ltd.
April 2011

APPENDIX G

RESISTIVITY DEPTH IMAGES (RDI)

Please see RDI Folder on DVD for the PDF's